Metabolomic Responses of Green Alga Chlamydomonas reinhardtii Exposed to Sublethal Concentrations of Inorganic and Methylmercury

Slaveykova, Vera; Majumdar, Sanghamitra; Regier, Nicole; Li, Weiwei; Keller, Arturo A.

How to cite

SLAVEYKOVA, Vera et al. Metabolomic Responses of Green Alga Chlamydomonas reinhardtii Exposed to Sublethal Concentrations of Inorganic and Methylmercury. In: Environmental Science & Technology, 2021, vol. 55, n° 6, p. 3876–3887. doi: 10.1021/acs.est.0c08416

This publication URL: https://archive-ouverte.unige.ch/unige:151639
Publication DOI: 10.1021/acs.est.0c08416

Metabolomic responses of green alga *Chlamydomonas reinhardtii* exposed to sub-lethal concentrations of inorganic and methylmercury

Vera I. Slaveykova[a,*], *Sanghamitra Majumdar*[b], *Nicole Regier*[a], *Weiwei Li*[b], *Arturo A. Keller*[b]

[a] University of Geneva, Faculty of Sciences, Earth and Environment Sciences, Department F.-A. Forel for Environmental and Aquatic Sciences, Environmental Biogeochemistry and Ecotoxicology, Uni Carl Vogt, 66 Blvd Carl-Vogt, CH 1211 Geneva, Switzerland

[b] Bren School of Environmental Science & Management, University of California, Santa Barbara, California 93106-5131, United States

*corresponding author: vera.slaveykova@unige.ch

This is the accepted version, the published version can be found at:
https://pubs.acs.org/doi/abs/10.1021/acs.est.0c08416

ABSTRACT

Metabolomics characterizes low-molecular-weight molecules involved in different biochemical reactions and provides an integrated assessment of the physiological state of an organism. By using a liquid chromatography - mass spectrometry targeted metabolomics, we examined the response of green alga *Chlamydomonas reinhardtii* to sub-lethal concentrations of inorganic mercury (IHg) and monomethylmercury (MeHg). We quantified the changes in the levels of 93 metabolites pre-selected based on the disturbed metabolic pathways obtained in a previous transcriptomics study. Metabolites are downstream products of the gene transcription; hence, metabolite quantification provided information about the biochemical status of the algal cells exposed to Hg compounds. The results showed that alga adjusts its metabolism during 2h-exposure to 5×10^{-9} and 5×10^{-8} mol L^{-1} IHg and MeHg by increasing the level of various metabolites involved in amino acid and nucleotide metabolism, photorespiration and TCA cycle, as well as metabolism of fatty acids, carbohydrates and antioxidants. Most of the metabolic perturbations in the alga were common for IHg and MeHg treatments. However, the exposure to IHg resulted in more pronounced perturbations in fatty acid and TCA metabolism as compared with exposure to MeHg. The observed metabolic perturbations were generally consistent with our previously published transcriptomics results for *C. reinhardtii* exposed to the comparable level of IHg and MeHg. The results highlight the potential of metabolomics for toxicity evaluation, especially to detect effects at an early stage of exposure prior their physiological appearance.

KEYWORDS: targeted metabolomics, inorganic mercury, methylmercury, phytoplankton, mode of action

SYNOPSIS: Targeted metabolomics detect early on metabolic alterations in algae exposed to sublethal mercury species concentrations that can later express physiologically.

40 GRAPHICAL TABLE OF CONTENT

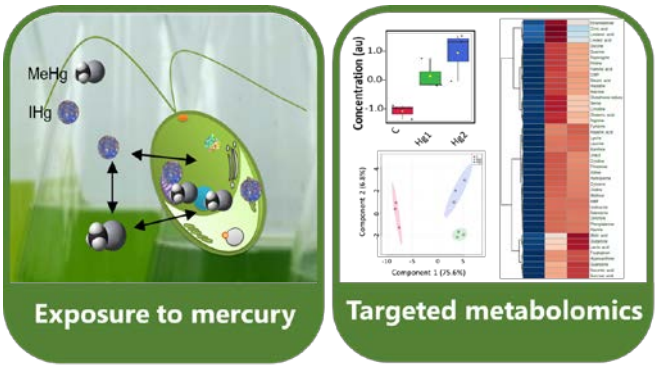

41

INTRODUCTION

Advances in 'omic' technologies has opened novel avenues in ecotoxicology research towards elucidating contaminant modes-of-action, biomarker discovery and predictive risk assessment [1, 2]. Metabolomics, the youngest among the 'omic' technologies, characterizes low-molecular-weight metabolites involved in different biochemical reactions and captures the cellular status and physiological state of an organism [3-6]. Existing advancements in environmental metabolomics, in particular chemical stressors induced metabolic perturbation in different organisms, including fish and invertebrates [7, 8], plants [9, 10] and microalgae [11] were comprehensively reviewed. However, relatively few studies have explored contaminant-induced metabolic perturbations in phytoplankton to address ecotoxicological questions. In the specific case of toxic metals, such as Ag, Cd, Cu, Pb, Zn, only a few metabolomic studies with green algae, diatoms or cyanobacteria have been carried out [6, 11-13]. Based on a literature search (keywords mercury and metabolomics and algae), no studies exist dealing with metabolomics response of algae exposed to Hg, a priority contaminant of global importance.

The present study focusses on Hg as characterized with high persistence, bioaccumulative and biomagnifying potential [14]. The toxicity of Hg towards living beings is well known [15]; however, the metabolomic response is not well understood. There has been progress in overall understanding of the adverse effects of Hg, including at the molecular level, with comprehensive reviews for animal cells, invertebrates and vertebrates [16], phytoplankton [17, 18] and aquatic plants [19, 20]. However, these previous studies focused on distinct effects or do not cover the level of resolution we are considering in this study. The physiological and transcriptomic responses in green alga *Chlamydomonas reinhardtii* during short-term exposure to inorganic mercury (IHg) and monomethylmercury (CH_3Hg^+, MeHg), two mercury species prevailing in the aquatic

environments, were assessed [21-23]. These studies demonstrated that multiple metabolic pathways could be disturbed by IHg and MeHg including those related to dysregulation of antioxidants, detoxification, energy resources, etc. [21-23]. However, transcriptomics provides only a partial understanding of the cellular response given that not all genes that are transcribed are translated into functional gene products [24]. As downstream products of the gene transcription and protein expression, metabolites provide information about the biochemical status of the algal cells exposed to Hg compounds.

In such a context the primary goal of the present study was to further examine the responses of green alga *C. reinhardtii* to sub-lethal concentrations of IHg and MeHg by using targeted metabolomics in order to obtain novel insights into the molecular basis underlying the cellular responses to mercury compounds. Liquid chromatography-mass spectrometry (LC-MS) targeted metabolomics was employed to quantify over 93 metabolites preselected based on the disturbed metabolic pathways determined by transcriptomics [22]. Targeted metabolomics was chosen as providing the advantage of more sensitive and accurate detection of predetermined metabolites [25]. The metabolomics results were compared with the physiological response and transcriptomics study from our previous work [22].

MATERIAL AND METHODS

Chemicals and labware

All the labware material was pre-washed in 10% HNO_3 (EMSURE, Merck, Darmstadt, Germany) followed by 10% HCl acid bath (EMSURE, Merck, Darmstadt, Germany) for 2h under sonication, thoroughly rinsed with ultrapure water (MilliQ Direct system, Merck, Darmstadt, Germany) and

subsequently autoclaved for sterilization. $HgCl_2$ (IHg) and CH_3HgCl (MeHg) standard solutions (1.0 g L^{-1}) were purchased from Sigma-Aldrich, Buchs, Switzerland.

Culture conditions and exposure to mercury compounds

Green alga *Chlamydomonas reinhardtii* CPCC11 (Canadian Phycological Culture Centrer, Waterloo, Canada) was axenically grown in 4× diluted Tris-Acetate-Phosphate medium [26] at 20.2 ± 0.5°C, 115 rpm and 12:12h light: dark cycle in a specialized incubator (Multitron Infors HT, Bottmingen, Switzerland). At mid-exponential growth phase, the algal cultures were isolated from the growth medium by gentle centrifugation (4°C 10 min, 1300 g), rinsed and re-suspended in the exposure medium. The exposure medium contained 8.2×10^{-4} mol L^{-1} $CaCl_2\cdot2H_2O$, 3.6×10^{-4} mol L^{-1} $MgSO_4\cdot7H_2O$, 2.8×10^{-4} mol L^{-1} $NaHCO_3$, 1.0×10^{-4} mol L^{-1} KH_2PO_4 and 5.0×10^{-6} mol L^{-1} NH_4NO_3, adjusted to pH 7.0 ± 0.1. Given the dependence of the algal metabolic state on the growth phase [27] and the light and dark cycle [28], the experiments were performed with cells sampled exactly at the same growth stage (68h), 4h after the light in the incubator was switched on. For each test, the algal cells were re-suspended in exposure medium to a final density of 4×10^6 cells·mL^{-1} in the absence (unexposed control, C) and presence of IHg or MeHg with a nominal concentration of 5×10^{-9} (IHg1) and 5×10^{-8} mol L^{-1} (IHg2) of IHg or 5×10^{-9} mol L^{-1} (MeHg1) or 5×10^{-8} mol L^{-1} (MeHg2) of MeHg. Cell density was determined using a Coulter counter (Beckman Coulter Counter).

To enable comparison with already published transcriptomics and physiological effects results [22], an exposure duration of 2h was selected. Exposures and analysis were performed on three independent biological replicates. At the end of the exposure period, the microorganisms were centrifuged for 10 min at 1300 g. The supernatant was discarded and the pellet deployed in liquid

nitrogen to stop the metabolic activities. The pellets were kept at -80°C overnight and then freeze-dried (Beta 1-8 K, Christ, Germany).

Determination of mercury concentrations in the exposure medium and algal cells

The cellular concentration of total mercury (THg = IHg+MeHg) in *C. reinhardtii* was determined from the freeze-dried pellets by atomic absorption spectrometry using a Direct Mercury Analyzer DMA-80 (Milestone, USA). The accuracy of the measurements was followed by certified reference material (CRM) MESS-3 from National Research Council of Canada, showing 100 ± 0.1 % recovery. The amount of THg accumulated by algal cells was expressed in mg kg^{-1} dry weight of algal biomass (**Fig. S1**, Supplementary information, SI). The concentrations of THg in the exposure medium were measured by using a MERX® Automated Total Mercury Analytical System (Brooks Rand Instruments, Seattle, WA, USA), with a detection limit of 1.5 $\times 10^{-13}$ mol L^{-1}. The accuracy of THg measurements by MERX® was tested by analyzing the CRM ORMS-5 (National Research Council of Canada, 116.0 ± 3.5% recovery). The measured concentrations of IHg in the exposure medium correspond to the nominal concentrations of 5×10^{-9} and 5×10^{-8} mol L^{-1} were (1.55 ± 0.01) $\times10^{-9}$ and (6.70 ± 0.60) $\times10^{-8}$ mol L^{-1} , respectively. For nominal concentration of $5x10^{-9}$ and 5×10^{-8} M MeHg, the measured concentrations were (3.70 ± 0.21) $\times10^{-9}$ and (6.59 ± 0.23) $\times10^{-8}$ mol L^{-1} , respectively.

All the results are reported as mean and standard deviation (SD), calculated from three independent experiments. One-way Analysis of Variance (ANOVA) was performed to test for significant differences between the treatments by the statistical module build in SigmaPlot 12.5. The Tukey Honestly Significant Difference (Tukey HSD) was performed as a post-hoc test. A $p < 0.05$ was considered statistically significant.

Liquid chromatography - mass spectrometry based targeted metabolomics

The metabolic alterations in green alga *C. reinhardtii* exposed to IHg or MeHg were determined by LC-MS based targeted metabolomics using Agilent 6470 liquid chromatography triple quadrupole mass spectrometer (Agilent Technologies, USA) as previously described [29-31]. Ninety-three metabolites, including antioxidants, amines, amino acids, organic acids/phenolics, nucleobase/side/tide, sugar/sugar alcohols and fatty acids, were extracted following previously developed methodology [13, 29, 30]. The list of considered metabolites was the same as in our previous study [13] and is provided in **Table S1** together with their measured limit of detection (MDLs).

Statistical and pathway analyses of the metabolomics data were performed for controls, IHg and MeHg exposures using MetaboAnalyst 4.0 [32, 33]. First, the data were corrected for batch effect using the built-in module for MetaboAnalyst, based on the ComBat method [34]. Next, one-way Analysis of Variance (ANOVA) followed by Fisher's LSD post-hoc analysis with $p < 0.05$ was completed to screen for metabolites differing in concentration between Hg treatments and controls. Unsupervised Principal Component Analysis (PCA) and supervised Partial Least Squares - Discriminant Analysis (PLS-DA) were performed to get a global overview of the metabolic changes. Metabolites with a Variable Importance in the Projection (VIP) greater than 1 were regarded as significant and responsible for group separation [35]. Metabolite concentrations were not subjected to any further normalization or transformation.

Metabolites significantly dysregulated by the respective Hg treatments, as identified via ANOVA and PLS-DA, were further considered in the pathway analysis to identify the most relevant pathways altered by sublethal levels of IHg or MeHg. Pathway enrichment and pathway topology

analyses were performed with MetaboAnalyst 4.0 [32, 33] with respect to KEGG pathway built-in metabolic library of green alga *Chlorella variables* [33]. Over-representation analysis was performed using Fisher's exact test. The pathway topology analysis uses the node centrality measure to estimate node importance was "betweenness centrality". Pathways with threshold > 0.1 were considered as significantly dysregulated [32, 36].

RESULTS AND DISCUSSION

Overview of metabolic profiles in *C. reinhardtii* exposed to IHg and MeHg

Of a total of 93 metabolites analyzed, 52 were detected above their MDLs (**Table S1**) and quantified in the controls, IHg and MeHg treatments. A general overview of the treatment clustering was obtained by the unsupervised PCA and supervised PLS-DA methods. The PCA and PLS-DA score plots for IHg (**Fig. 1**) and MeHg (**Fig. 2**) treatments showed a good separation between the Hg treatments and untreated control. Based on a VIP score >1, 30 responsive metabolites were subsequently employed to distinguish the untreated controls from IHg treatments (**Fig. S2**). After comparing the IHg-treatments to the untreated control by ANOVA, 15 additional metabolites were identified as significantly dysregulated (**Table S2**). All the 45 responsive metabolites were upregulated by Hg-treatments in comparison with untreated control (**Fig. 1C**), however the intensity of the dysregulation was concentration dependent. For the MeHg treatments, a total of 39 responsive metabolites were identified via VIP score and ANOVA, after comparison to the untreated controls (**Figs. 2C, S3, Table S3**). All of them increased levels upon MeHg treatments as compared with the untreated control, but the relative metabolite abundance was dose-dependent.

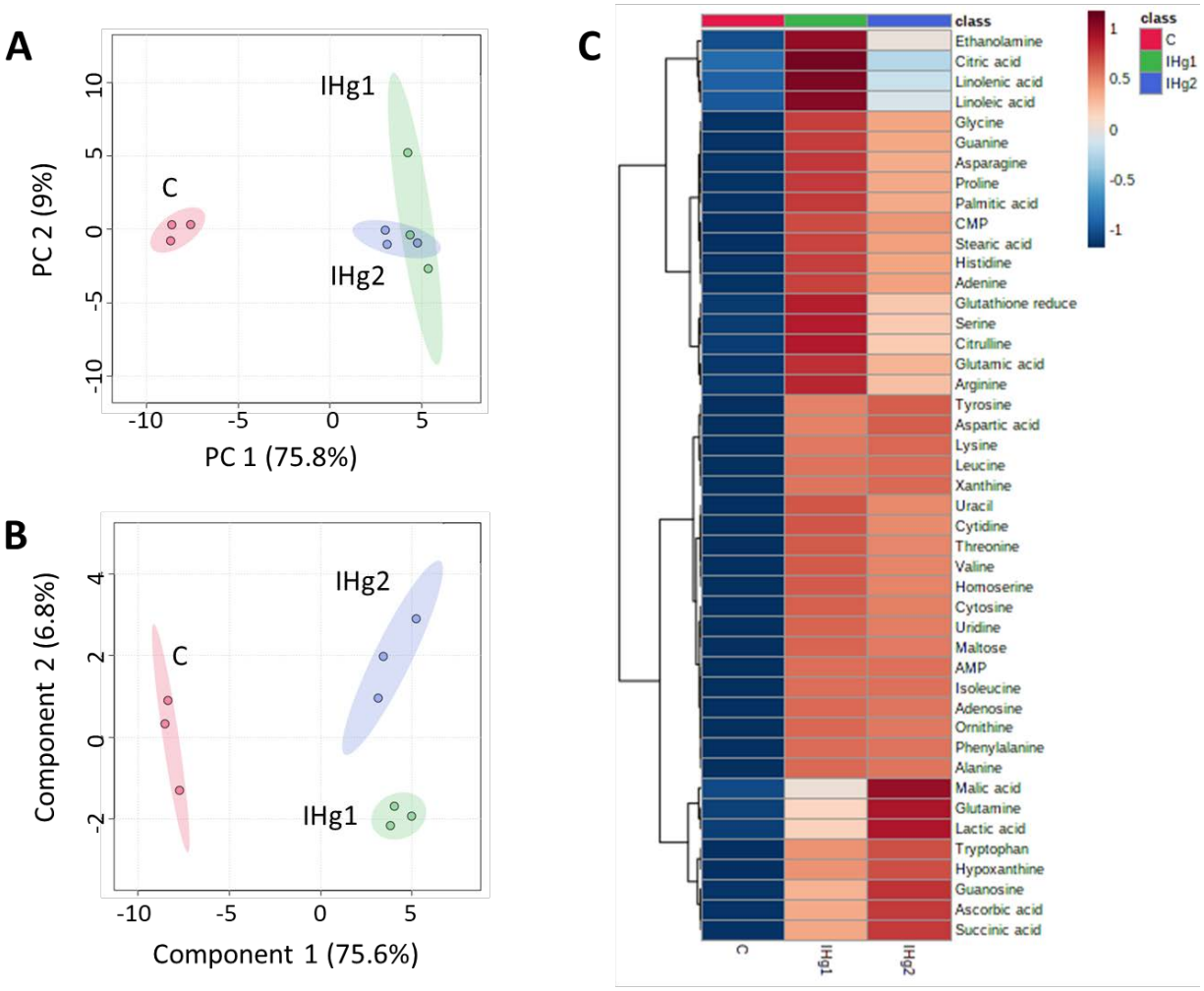

Figure 1. Analysis of metabolic response of *C. reinhardtii* treated with 2h with 5×10^{-9} mol L^{-1} IHg (IHg1), 5×10^{-8} mol L^{-1} IHg (IHg2): (A) principal component analysis (PCA); (B) partial least-squares discriminate analysis (PLS-DA) score plots. (C) Clustering metabolites and samples shown in a heat map (Euclidean distance and Ward clustering algorithm). Data were not normalized or transformed, but were autoscaled.

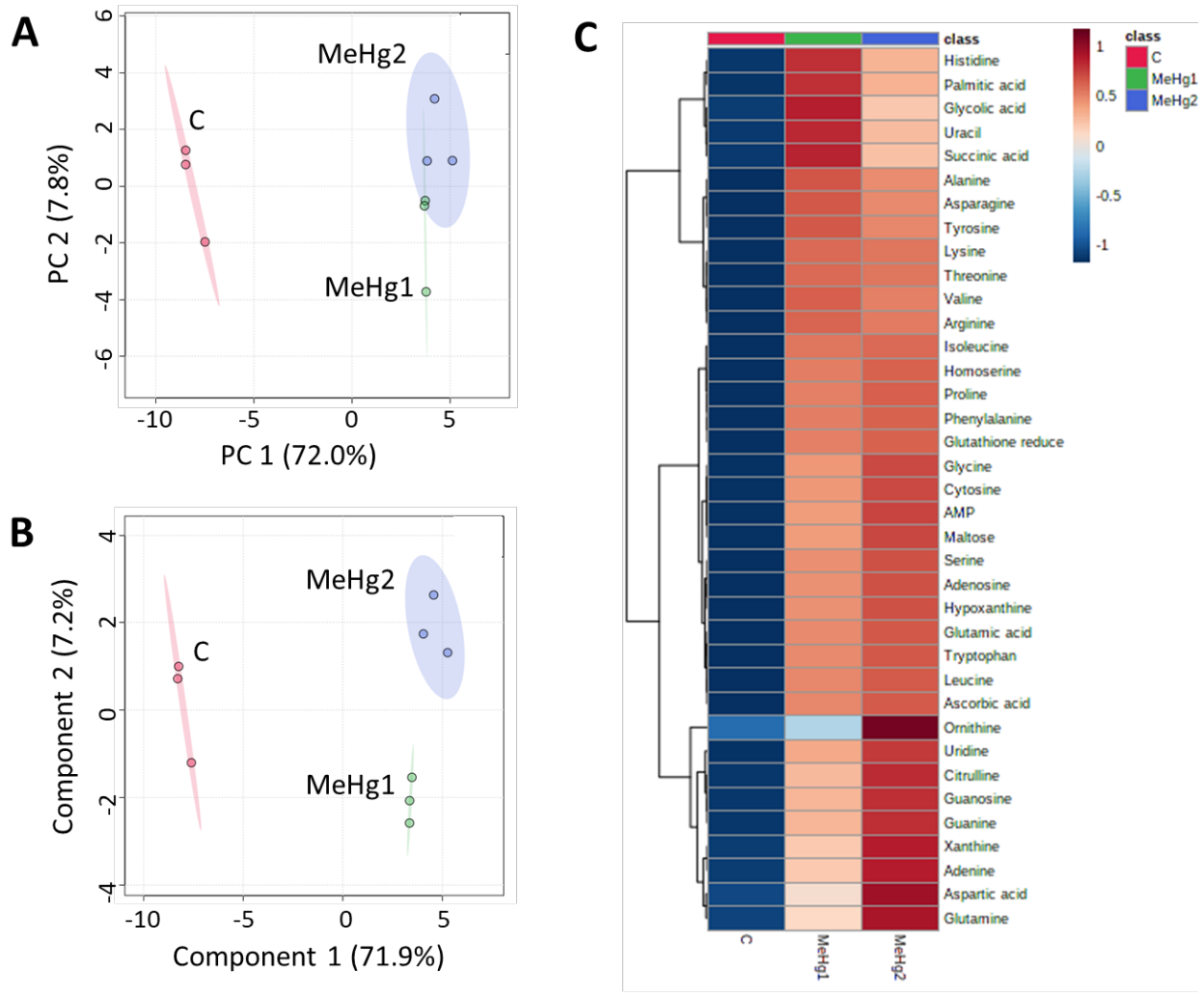

Figure 2. Analysis of metabolic response of *C. reinhardtii* treated for 2h with 5×10^{-9} mol L^{-1} MeHg (MeHg1), 5×10^{-8} mol L^{-1} MeHg (MeHg2); unexposed control (C). (A) Principal component analysis (PCA), (B) partial least-squares discriminate analysis (PLS-DA) score plots. (C) Clustering metabolites and samples shown in a heat map (Euclidean distance and Ward clustering algorithm). Data were not normalized or transformed, but were autoscaled.

Heatmap clustering served to group the quantified responsive metabolites (**Figs. 1C and 2C**). Globally 3 large groups were obtained. Group 1 corresponded to metabolites accumulated more strongly at lower Hg-concentrations (18 for IHg and 5 for MeHg). Group 2 included metabolites with comparable abundances at the two concentrations (18 for IHg and 12 for MeHg, no concentration dependence). Group 3 encompassed metabolites accumulated to a larger degree at higher IHg or MeHg concentrations (8 for IHg ad 20 for MeHg).

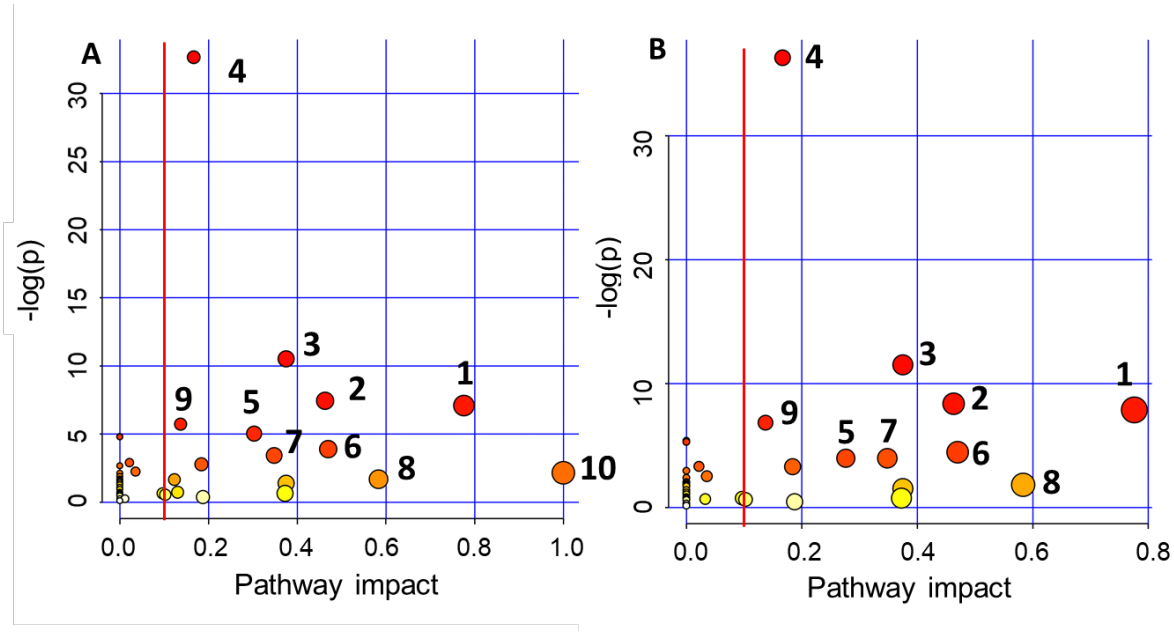

Figure 3. Pathway analysis for metabolites with altered abundance in *C. reinhardtii* exposed to (A) IHg and (B) MeHg. The node color is based on its p-value and changes from red to yellow with the increase of p-value. The node size reflects the pathway impact values, with bigger nodes corresponding to high impact values. Affected pathways: 1: Alanine, aspartate and glutamate metabolism, 2: Glycine, serine and threonine metabolism, 3: Arginine biosynthesis, 4: Aminoacyl-tRNA biosynthesis, 5: Glyoxylate and dicarboxylate metabolism, 6: Glutathione metabolism, 7: Arginine and proline metabolism. 8: Isoquinoline alkaloid biosynthesis, 9: Purine metabolism; 10:

Linoleic acid metabolism. 45 responsive metabolites for IHg and 39 for MeHg obtained in algal treatments with 5×10^{-9} and 5×10^{-8} mol L^{-1} IHg or MeHg were used for the pathway analysis.

The responsive metabolites identified by PLS-DA and ANOVA corresponded to 15 and 13 impacted pathways in IHg and MeHg treatments, respectively (**Figs. 3** and **S4, Tables S4** and **S5**, impact threshold 0.1). The top 5 most impacted pathways by sublethal concentration of both IHg and MeHg included: (1) alanine, aspartate and glutamate metabolism; (2) glycine, serine and threonine metabolism; (3) arginine biosynthesis; (4) glutathione metabolism; and (5) isoquinoline alkaloid biosynthesis. These results confirmed previous findings via transcriptomics that IHg and MeHg altered similar pathways in *C. reinhardtii* [21, 22]. In addition, alpha-linolenic acid metabolism was significantly affected only by IHg exposure (**Tables S4**, **Fig. 3A**).

Metabolic perturbation in *Chlamydomonas reinhardtii* exposed to sub-lethal levels of IHg and MeHg

Amino acids metabolism: Exposure to IHg and MeHg induced a significant dysregulation of amino acid metabolism of *C. reinhardtii* (**Figs. 4-6**). Amino acids represent structural units of the proteins and polypeptides, as well as serve as precursors for the synthesis of various metabolites with multiple functions in algal growth and other biological processes [37-39]. A significant increase ($p < 0.05$) in the relative abundance of 21 amino acids was observed in both IHg and MeHg treatments, implying an acceleration of the amino acid synthesis and/or degradation of proteins, as well as an active defense of *C. reinhardtii* from the stress induced by Hg compounds. As amino acids are part of the aminoacyltRNA biosynthesis, the increase in their abundance suggests that the exposure to both IHg and MeHg affect the synthesis of proteins that are central to

algal growth. Similarly, the aminoacyltRNA biosynthesis in the aquatic plant *Elodea nuttalli* was affected by exposure to Cd and MeHg [40].

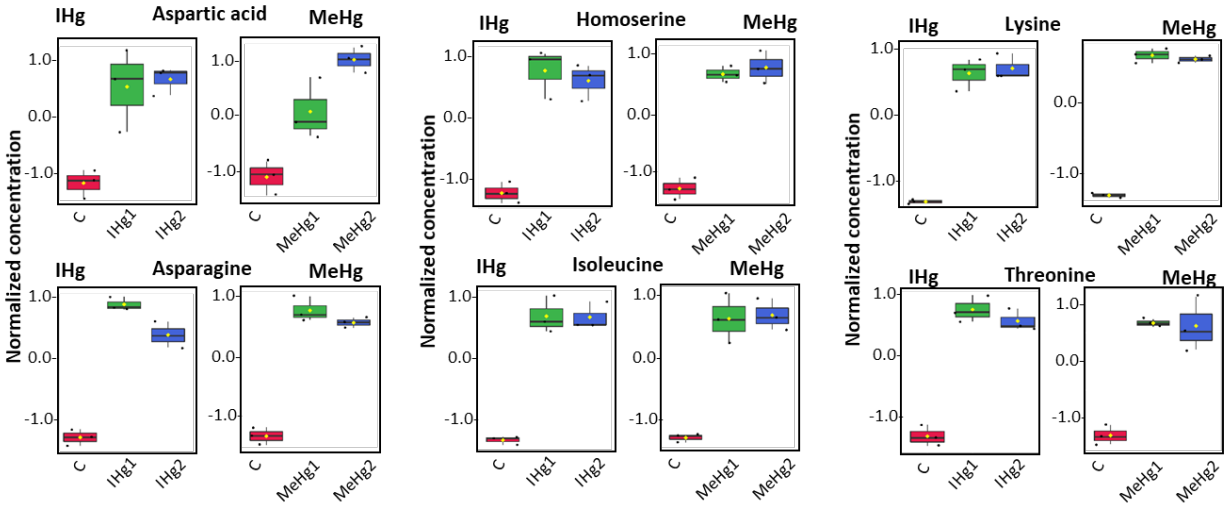

Figure 4. Box plots of relative abundance of oxaloacetate-derived amino acids: aspartate, asparagine, homoserine, isoleucine, lysine, threonine. *C. reinhardtii* was treated for 2h with 5×10^{-9} mol L^{-1} IHg (IHg1), 5×10^{-8} mol L^{-1} IHg (IHg2), 5×10^{-9} mol L^{-1} MeHg (MeHg1), 5×10^{-8} mol L^{-1} MeHg (MeHg2); unexposed control (C).

Aspartate, generated by transamination of oxaloacetate, a tricarboxylic acid cycle (TCA) cycle intermediate, accumulated in cells exposed to IHg and MeHg. *Aspartate* serves as a precursor for the biosynthesis of other amino acids: *asparagine*, *homoserine*, *threonine*, *lysine*, and *isoleucine* [39], which were also accumulated (**Fig. 4**). This finding is in line with our previous transcriptomics study [22] showing that several genes driving the synthesis of amino acids were downregulated after exposure to IHg and MeHg (ASK1 coding for aspartate kinase; DPS1 gene for dihydrodipicolinate synthase and HSK1 for homoserine kinase (thrB1) and AAD1 for

acetohydroxyacid dehydratase. The ASNS gene that codes for asparagine synthase, which catalyzes amidation of aspartate to asparagine, was down-regulated in the MeHg treatment [22]. The down regulation of genes may be a compensatory response to the accumulation of amino acids. Indeed, metabolites are not only the final product of gene transcription, but also can regulate gene transcription.

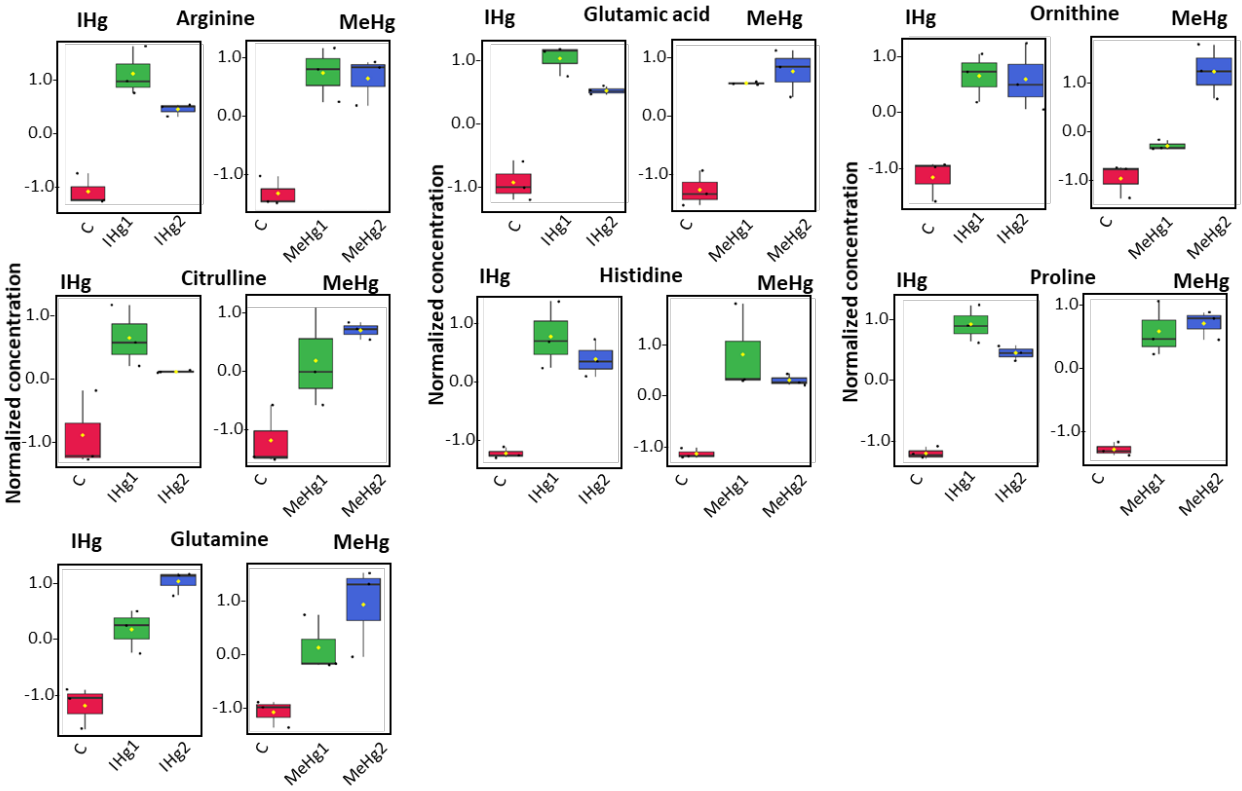

Figure 5. Box plots of relative abundance of α-ketoglutarate derived amino acids: arginine, citrulline, glutamate, glutamine, ornithine, histidine, proline. *C. reinhardtii* was treated for 2h with 5×10^{-9} mol L^{-1} IHg (IHg1), 5×10^{-8} mol L^{-1} IHg (IHg2), 5×10^{-9} mol L^{-1} MeHg (MeHg1), 5×10^{-8} mol L^{-1} MeHg (MeHg2); unexposed control (C).

Glutamate, glutamine, ornithine, citrulline, arginine and histidine biosynthesized from the TCA metabolite α-ketoglutarate [41] increased in cells exposed to both IHg and MeHg (**Fig. 5**). Glutamine is part of the glutamine-glutamate cycle responsible for ammonia assimilation by *C. reinhardtii* [39]. The present findings are consistent with our previous transcriptomics results showing that genes GLN1, coding for glutamine synthetase and GSF1, coding for ferredoxin-dependent glutamate synthase were significantly upregulated in the MeHg treatment [22]. However, gene GDH1, coding for the glutamate dehydrogenase 2, which catalyzes the synthesis of glutamate from ammonium, was significantly down regulated in the MeHg treatment [22]. The assimilation of ammonia to glutamine and glutamate is catalyzed by the enzymes, glutamine synthetase, glutamate synthase and glutamate dehydrogenase. Glutamine synthetase also plays an important role in nitrate assimilation [42]. Therefore, these results suggest that assimilation of ammonia and nitrate are likely to be accelerated, supporting the finding that the levels of amino acids have been increased.

The increase in the abundance of *histidine* observed in this study was consistent with significant down-regulation of several genes coding for enzymes involved in different steps of histidine biosynthesis, as observed in MeHg exposures in our previous study [22]: RPPK1-ribose-phosphate pyrophosphokinase; HDH1-histidinol dehydrogenase), HIS3- imidazoleglycerol-phosphate dehydratase. Histidine is an amino acid needed for growth and development of algal cells, therefore the accumulation observed here reveals an influence of Hg-treatments on algal growth and cell development.

Proline plays an important role in osmo- and redox-regulation, metal chelation, and scavenging of free radicals induced by different metals, including Hg in plants [43, 44]. Proline accumulation in

cells exposed to IHg and MeHg could be a defense response to oxidative stress as well as enable Hg complexation. As in plants, there are two alternative pathways in *C. reinhardtii* that are involved in the proline biosynthesis: direct glutamate pathway and ornithine pathway, where glutamate is first converted to ornithine [39]. In our previous studies, PCR1 gene - pyrroline-5-carboxylate reductase was upregulated in *C. reinhardtii* after exposure to MeHg [22]. The PCR1 encodes the enzyme Δ 1-pyrroline-5-carboxylate reductase, which controls the conversion of Δ 1-pyrroline-5-carboxylate to proline by the NADPH [39].

Alanine, leucine and valine are biosynthesized from pyruvate, a common metabolite of intermediary metabolism [39]. They were significantly accumulated in Hg-exposed cells (**Fig. 6A**). *Alanine* can be synthesized by reversible transamination of pyruvate with glutamate which is catalyzed by alanine aminotransferase (AAT). The gene coding for AAT1 alanine aminotransferase is upregulated in IHg and MeHg treatments [22]. AAT is thought to play a role in photorespiration, because of the ability of AAT to transaminate glyoxylate to glycine using glutamate as an amino donor [39]. Pyruvate also can be transaminated to alanine, a process catalyzed by alanine-glyoxylate aminotransferase (AGT1), but it is not considered to have a significant role in alanine synthesis [39]. Interestingly the gene AGT1, coding for alanine-glyoxylate aminotransferase, was upregulated significantly only in MeHg treatment, not in IHg. The gene BCA1 coding for branched chain amino acid aminotransferase, involved in the biosynthesis of leucine from pyruvate, was upregulated in both IHg and MeHg treatments [22]. *Leucine* serves as an oxidative phosphorylation energy source [45]. The solely ketogenic amino acids, lysine, valine and leucine, will be converted to acetyl-CoA and will presumably be used as substrate for the TCA cycle or contribute to pools for fatty acid synthesis [46]. Using a *Chlamydomonas reinhardtii* mutant

bkdE1α, it was shown that leucine, isoleucine and valine, amino acids with a branched aliphatic chain, contribute to triacylglycerol metabolism by providing carbon precursors and ATP [47]. Indeed, leucine, isoleucine and valine and their degradation products were shown to include an acetyl-CoA, potential substrates for de novo fatty acid synthesis [48].

Levels of aromatic amino acids, *phenylalanine, tyrosine and tryptophan*, derived from phosphoenolpyruvate, were significantly enhanced in Hg treatments (**Fig. 6B**). Phenylalanine and tyrosine are precursors for the synthesis of pigments, including the carotenoids and PQ, respectively, via coumarate and acetoacetyl CoA [49]. Carotenoids are bound to the protein complexes of the photosystem I and II of *C. reinhardtii* and known to protect the photosynthetic apparatus against photo-oxidative damage [50]. Therefore, the increase levels of phenylalanine and tyrosine suggest the acceleration of biosynthesis of carotenoids and enhanced cellular defense mechanisms. The accumulation of these amino acids concorded with previously observed down-regulation of multiple genes involved in their biosynthesis, in particularly in MeHg treatments [22]. For examples AGD1 gene coding for arogenate/prephenate dehydrogenase; PRD1 and TSA for tryptophan synthetase alpha subunit were downregulated in MeHg exposure [22].

Concentrations of two other amino acids, *glycine and serine*, were significantly increased by exposure to both IHg and MeHg (**Fig. 6C**). Usually these amino acids are synthesized by the photorespiratory glycolate cycle in algae [39], so their accumulation could be interpreted as acceleration of the photorespiratory activity, probably to produce the energy required for the synthesis of different defense components needed to cope with the stress induced by Hg-treatments. This correlates well with the observed accumulation of glycolate (**Fig. S5**), a photorespiratory intermediate. Photorespiration is one of the major carbon metabolism pathways in photosynthetic organisms [51], therefore the present results could indicate an acceleration of the C- metabolism of

C. reinhardtii due to IHg and MeHg exposure. The possible acceleration of photorespiration is consistent with upregulation in MeHg treatment of the RBCS gene (coding for ribulose-1,5-bisphosphate carboxylase/oxygenase, which catalyzes carbon fixation to phosphoglicolite and the PGP1 gene coding for phosphoglycolate phosphatase/4-nitrophenylphosphatase involved in phosphoglycolate to glycolate conversion [22]. Possible acceleration of the photorespiratory glycolate cycle and consequent increase of the serine concentration also corroborate with the upregulation of the SHMT1 and SGA1 genes after exposure to IHg and MeHg [22]. SGA1coding for serine glyoxylate aminotransferase to catalyze the conversion of glyoxylate to glycine via serine. In addition, SHMT1 gene coding for serine hydroxymethyltransferase which catalyze the second step of the serine synthesized from two molecules of glycine in a two-step process via the glycine decarboxylase complex and serine hydroxymethyltransferase [39]. However the ratios of glycine to serine, used as indicators of photorespiratory activity [52], were comparable in IHg-exposure (IHg1: 0.56 ± 0.04; IHg2: 0.63 ± 0.08), MeHg exposure (MeHg1: 0.55 ± 0.04; MeHg2: 0.57 ± 0.09) and in unexposed control (C: 0.56 ± 0.10). Glycine and serine can be also synthesized by a non-photorespiratory pathway, phosphorylated pathway [39], which could probably be accelerated. The phosphorylated serine pathway is catalyzed by the PGD1, PST1, and PSP1 enzymes, however the gene coding for D-3-phosphoglycerate dehydrogenase (PGD1), for phosphoserine aminotransferase (PST1) and phosphoserine phosphatase (PSP1) were not among the significantly dysregulated genes in IHg and MeHg exposure [22]. These findings are in line with the increase in the maximum photosynthetic yield in MeHg-treatments (**Fig. S6**).

The accumulation of numerous amino acids could also contribute to chelation of Hg^{2+} and CH_3Hg^+ ions inside the cells [44]. The results from this study are consistent with published studies demonstrating an accumulation of free amino acids in green alga *Scenedesmus vacuolatus* exposed to prometryn [53], *Chlorella vulgaris* to boscalid [54] and *Dunaliella tertiolecta* to diuron [55].

Such an accumulation suggests alteration of the energy metabolism associated with an activation of catabolic processes and use of protein for energy supply [11]. An increase in amino acid pools under stress conditions has been also reported in sulfur depleted *C. reinhardtii* cells [56] and in *C. reinhardtii* under hyperosmotic stress [57]. However the present finding for IHg and MeHg are opposite to the decrease of some of the amino acid (lysine, arginine, and glutamine) observed in copper exposure of other green alga *Chlorella* sp. [58, 59], *Scenedesmus quadricauda* [60] and diatom *Tabellaria flocculosa* (Roth) Kützing [61].

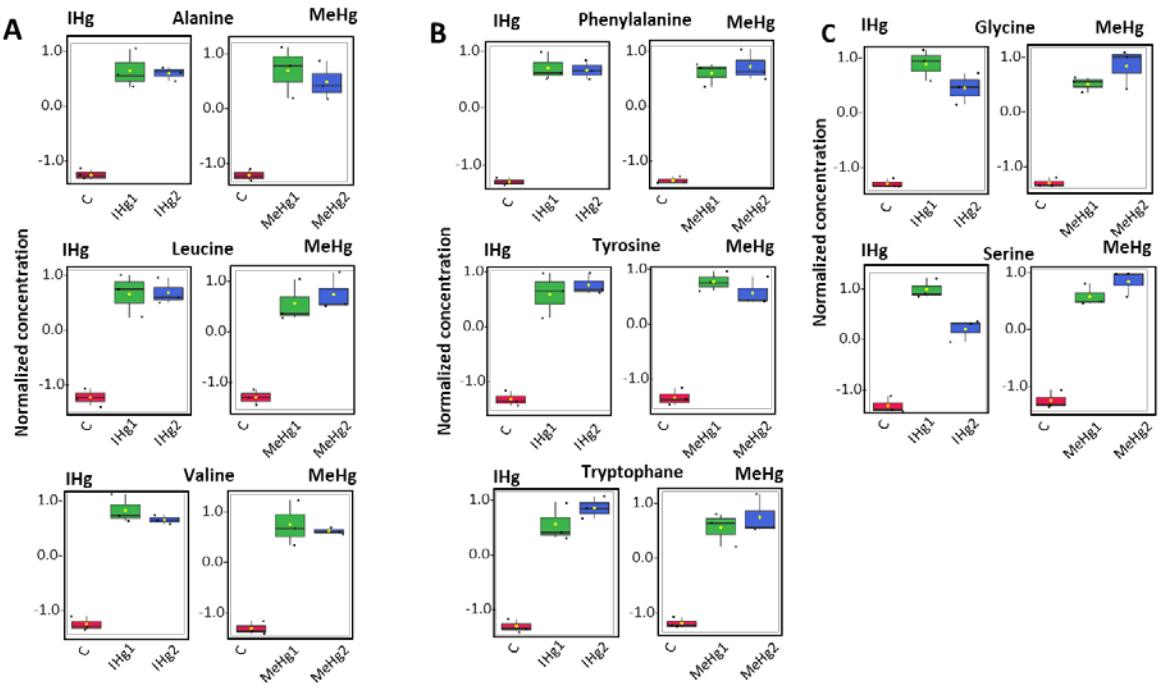

Figure 6. Box plots of relative abundance of (A) Pyruvate - derived amino acid, alanine, leucine and valine; (B) phosphoenolpyruvate derived amino acids, phenylalanine, tyrosine and tryptophan; and (C) glycine and serine. *C. reinhardtii* was treated for 2h with 5×10^{-9} mol L^{-1} IHg (IHg1), $5\times10^{-}$

^{8}mol L^{-1} IHg (IHg2), 5×10^{-9} mol L^{-1} MeHg (MeHg1), 5×10^{-8} mol L^{-1} MeHg (MeHg2); unexposed control (C).

Nucleobase/tide/side metabolism: Metabolism of both pyrimidine and purine derivatives was significantly affected in algae exposed to IHg and MeHg (**Figs. S7 and S8**). The *pyrimidine* nucleobases, *cytosine* and *uracil,* significantly increased, as well as the corresponding nucleotides/sides *CMP* and *uridine*. Interestingly, the levels of these metabolites were greater at lower IHg concentration (IHg1) than at higher exposure (IHg2), whereas in the MeHg exposure their relative abundance increased with exposure concentration. The above observation is consistent with the increase of glutamine and aspartate, amino acids used for biosynthesis of the uridine monophosphate (UNP) and cytidine monophosphate (CMP) nucleotides. The thymidine monophosphate (TMP) metabolism seems unaffected by Hg - treatments. Pyrimidine nucleotides are involved in the synthesis of glycogen and phospholipids which seems to accelerate due to exposure to mercury [62]. CMP accumulation is consistent with upregulation, for MeHg treatments, of the genes coding for CDP-Ethanolamine:DAG Ethanolamine phosphotransferase which catalyzes the conversion of CDP-choline and 1,2-diacylglycerol to CMP and α phosphatidylcholine [22].

The *purine* metabolites (*AMP*, *adenosine*, *adenine*, *hypoxanthine*, *xanthine*, *guanosine* and *guanine),* significantly accumulated in algae exposed to both IHg and MeHg as compared with unexposed controls (**Fig. S8**). However, their abundances increased with exposure concentration only for MeHg. No significant changes in the abundance of other nucleobases / tides / sides such as IMP, GMP and inosine were observed. Such nucleobase accumulation after Hg treatments could

be related to an acceleration of their synthesis, a respective nucleoside/nucleotide degradation and salvaged for reincorporation into nucleotides. Indeed, the DNA and RNA could be hydrolyzed by nucleases to yield a mixture of polynucleotides, which are transformed to mononucleotides. They are further converted by the nucleosidases to nucleosides, which undergo phosphorolysis to yield the nucleobase. In our previous study, FAP215 gene coding for nucleotidase and flagellar associated protein was down regulated in both IHg and MeHg treatment [22] in agreement with the accumulated nucleosides (adenosine, guanosine, and hypoxanthine).

The above results indicate a significant upregulation of the pyrimidine and purine metabolism of *C. reimhardtii* by exposure to sublethal MeHg and IHg concentrations. Pyrimidine and purine nucleotides are structural units of the nucleic acids DNA and RNA [62]. Therefore, the present results suggest an acceleration of DNA and RNA synthesis and turnover. They are in good agreement with the amino acid upregulation, as the amino acids serve as precursors for a wide variety of metabolites including purine and pyrimidine nucleotides [39].

Antioxidant metabolism: Exposure to both IHg and MeHg led to a significant increase of *reduced glutathione (GSH)* after Hg-treatments (**Fig. S5**). Since GSH is central to redox control in the cell [63], this finding suggests an activation of the defense mechanism against the oxidative stress due to exposure to IHg and MeHg. GSH acts as redox buffer for the protection of cells against reactive oxygen species (ROS) produced by Hg [17]. Indeed, no significant generation of the ROS or membrane damage were found in *C. reinhardtii* exposed to IHg and MeHg (**Fig. S6**). GHS is a precursor of phytochelatins (-Glu-Cys)n-Gly with n = 2–11, PCn) synthesis, which is activated by different toxic metals including Hg [64]. PCn are considered major intracellular chelators for Hg detoxification [17]. GSH is also an important metal chelator in plant cells, and may also contribute to Hg detoxification [65]. Indeed, GSH is an important thiol involved in Hg sequestration in green

algae [66]. However, exposure to IHg resulted in a significant decline in GSH cellular concentrations in other green algae, such as *Cosmarium conspersum* and *C. autotrophica* [67]; it may reflect consumption of GSH after the interaction with ROS. In this study, for a comparable exposure concentration, IHg induced a significant depletion of GSH in comparison with MeHg, suggesting higher potency of IHg to induce PCn than MeHg. This is in line with existing literature, showing formation of IHg–phytochelatins complexes in green alga [68] and lower PCn induction capability of MeHg in the diatom cells [69]. GHS concentration in *C. reinhardtii* decreased during exposure to Cu [70, 71], whereas Cd exposure increased GHS concentrations as an antioxidant response by cells [71, 72]. The increase in GSH observed here is consistent with the previously observed upregulation of genes coding for glutathione peroxidase, an enzyme catalyzing the formation of glutathione disulfide (GS-SG) for GSH, MeHg (GPX3) and IHg (GPX5) treatments [22].

Ascorbic acid accumulated in *C. reinhardtii* cells after IHg and MeHg treatments. Ascorbic acid is a cellular antioxidant and it is involved in different cellular processes associated with photosynthetic functions and stress tolerance [73]. Increased concentrations of ascorbate could also play a role in preservation of the GSH pool and maintenance of the cellular redox balance by forming a primary barrier to ROS [73]. The accumulation of ascorbic acid showed that the antioxidant defense system of *C. reinhardtii* was activated by the IHg and MeHg treatments. Ascorbic acid is also known to play an important role in plant cell photoprotection [74].

Contrary to this finding, exposure to 10^{-4} mol L^{-1} IHg concentrations depleted ascorbic acid in the green alga *Coccomyxa subellipsoidea* [75], however the concentrations of IHg were 2×10^3 to 2×10^4 times higher than those used in the present study. Micromolar concentrations of IHg are known to induce rapid increase in ROS in the alga *Chlamydomonas* at micromolar doses [17, 76].

However, for IHg and MeHg concentrations comparable with those in the present work, no significant oxidative stress in *C. reinhardtii* was observed [22, 77]. The above results suggest that the algal cells limit ROS enhancement through an efficient antioxidant response at the metabolic level, well before the effects are observed physiologically.

Carboxylic acid metabolism: Three of the TCA intermediates (citric, succinic and malic acids) were significantly increased after IHg treatment (**Fig. S5**). The effect was more pronounced in IHg treatments, since for the MeHg treatments only the level of succinic acid was significantly enhanced. The changes in concentrations of citric and malic acids after MeHg treatment were not statistically significant ($p > 0.05$) (**Fig. S5**). Similarly to IHg exposure, the concentrations of citric, succinic and malic acids increased significantly in *P. malhamensis* exposed to Ag and AgNPs [13], as well as the level of malic acid in *Scenedesmus obliquus* exposed to AgNPs [78]. By contrast, a decrease in the TCA intermediates was observed in the diatom *Tabellaria flocculosa* exposed to high Cu concentrations [79]. As the TCA cycle is the core of the cell's respiratory machinery; it is likely that the increase in TCA intermediates observed here could be related to an increase in energy production necessary for the manufacture of defense compounds needed to cope with Hg-induced stress. The above findings are consistent with the observed alteration of genes involved in the TCA cycle [22]. Gene IDH3, coding for NAD-dependent isocitrate dehydrogenase, and NADP-dependent isocitrate dehydrogenase, which catalyzes the first carbon oxidation in the TCA cycle (i.e. oxaloacetate => 2-oxoglutarate), were down regulated by MeHg, but not IHg. The succinate to fumarate conversion is catalyzed by the succinate dehydrogenase succinate dehydrogenase 1-1 and succinate dehydrogenase both strongly down regulated by MeHg, whereas only succinate dehydrogenase 1-1 was down regulated in IHg treatments. MDH1 - NAD-dependent malate

462 dehydrogenase was down regulated by both IHg and MeHg treatments, whereas MDH2 - NADP-
463 dependent malate dehydrogenase, chloroplastic was upregulated in IHg and MeHg treatments.
464 Malate dehydrogenase is part of the second carbon oxidation, and catalyzes the conversion of 2-
465 oxoglutarate to oxaloacetate.

466

467 **Carbohydrates metabolism:** Of the 13 carbohydrates that were analyzed for, only three were
468 above detection limits and quantified: glucose/galactose, sucrose and maltose. Only the increase in
469 abundance of maltose was statistically significant ($p > 0.05$) in cells treated with IHg or MeHg.
470 *Maltose* is produced from starch and similar compounds in plants, and can be further hydrolyzed
471 to glucose by the enzyme maltase [80]. Maltose metabolism in plants is considered to make a
472 "bridge between transitory starch breakdown and the plants' adaptation to changes in
473 environmental conditions" [81]. Microalgae store fixed carbon as starch in their chloroplasts. As
474 needed, starch is converted to maltose and exported from the chloroplast to the cytosol where
475 maltose is converted to glucose, used as an energy source [82]. This suggest that algae exposed to
476 IHg or MeHg experience impaired carbohydrate biosynthesis. Accumulation of maltose and no
477 changes in the glucose abundance suggest that conversion of starch to maltose was accelerated as
478 an energy supply. This last suggestion is consistent with the upregulation of the MEX1 gene coding
479 for maltose exporter-like protein, MEX1, which was shown to be essential for starch degradation
480 in *C. reinhardtii* [83]. Similarly, AMYA1 alpha-amylase-like 3 gene was upregulated in *C.*
481 *reinhardtii* exposure to a comparable concentration of MeHg [22]. Taken together with the
482 alteration of the amino acid metabolism, TCA cycle and carbohydrates, this finding suggests the
483 activation of catabolic processes to restore energy balance in cells exposed to Hg-compounds.

484

Fatty acids metabolism: Among the 8 fatty acids considered, two saturated acids (i.e. *palmitic* (hexadecanoic acid, 16:0) and *stearic* (octadecanoic acid, 18:0) acids) and two unsaturated acids (i.e. *linolenic* (C 9,12,15 double bonds) and *linoleic* (C 9,12 double bonds) acids) accumulated in cells exposed to IHg (**Fig. S9**). After MeHg exposure only palmitic acid increased significantly, whereas the changes in the abundance of linoleic acid, linolenic acid, stearic acid were not significantly different from the unexposed control (all $p>0.05$). Similar changes in fatty acid composition have been frequently observed in algae under toxic metal stress [84]. Exposure to Cu resulted in an increase in the concentration of palmitic acid in *Tabellaria flocculosa* [79]. AgNPs and dissolved Ag induced an accumulation of linolenic acid, whereas arachidic and stearic acids were depleted in *P. malhamensis* [13]. Exposure to AgNPs and $AgNO_3$ reduced the abundance of monounsaturated and polyunsaturated fatty acids of the green microalga *Chlorella vulgaris* [85]. The results suggest that algae exposed to IHg , and in lower degree to MeHg, remodel the membrane fluidity to make it more tolerant to oxidation, thus preserving membrane integrity under oxidative stress conditions [86]. Indeed, palmitic acid is known to be less prone to oxidation than other fatty acids [86]. A perturbation of the metabolism of fatty acids could also change the cellular energy budget [87].

An increase in *ethanolamine* abundance was only observed in the IHg exposure, indicating alteration of the glycerophospholipid biosynthesis pathway by IHg. As glycerophospholipids are the main component of cell membranes, a decrease of those compounds can compromise membrane integrity. Opposite to the present finding, a decrease in ethanolamine was observed in other phytoplankton species such as *Chlorella* sp. exposed to copper [58].

Overall, the present targeted metabolomic study provides for the first-time information on the metabolic perturbations in green alga *C. reinhardtii* exposed to sub-lethal concentrations of IHg and MeHg and thus serves to improve biological understanding of the molecular basis of these

perturbations. The results revealed that the alga adjusts its metabolic state during exposure to IHg and MeHg, and accumulates metabolites involved in various metabolic pathways corresponding to amino acid and nucleotide synthesis and degradation, fatty acids, carbohydrates, TCA, antioxidants and photorespiration. Most of the observed metabolic perturbations were observed in both IHg and MeHg treatments. However, the exposure to IHg induced more pronounced perturbations in fatty acid and TCA metabolism than exposure to MeHg. The observed metabolic perturbations were generally consistent with previous transcriptomics results for *C. reinhardtii* exposed to IHg and MeHg. The results show that metabolites respond faster to IHg and MeHg exposure than algal physiology, and demonstrate the potential of metabolomics for toxicity evaluation, especially to identify biochemical markers and to detect effects at low toxicant levels and an early stage of exposure.

SUPPORTING INFORMATION

The Supporting Information is available free of charge at https://pubs.acs.org/

Cellular mercury content in alga *Chlamydomonas reinhardtii* (Fig. S1); VIP scores from PLS-DA analysis of discriminating metabolites between unexposed controls and IHg treatments (Fig. S2); VIP scores from PLS-DA analysis of discriminating metabolites between unexposed controls and MeHg treatments (Fig. S3); Metabolic pathways from KEGG with at least 2 significantly dysregulated metabolites by IHg or MeHg exposure (Fig. S4); Box plots of relative abundance of metabolites involved in carboxylic acid metabolism and antioxidants (Fig. S5); Effect of IHg and MeHg exposure on physiology of *C. reinhardtii*. (A) membrane damage assessed by PI stain and FCM; (B): ROS generation determined by CellRoxGreen stain and FCM; (C) chlorophyll a; (D) Maximum quantum yield of photosystem II (Fv/Fm) (Fig. S6); Box plots of relative abundance of nucleobase/tides/sides of pyrimidine metabolism (Fig. S7); Box plots of relative abundance of

nucleobase/tides/sides of purine metabolism (Fig. S8); Box plots of relative abundance of metabolites involved in fatty acids metabolism and ethanolamine (Fig. S9);

Measured metabolites and the MS parameters for LC-MS targeted metabolomics (Table S1); Important features identified by One-way ANOVA and Fisher's post-hoc analysis ($p< 0.05$) in *C. reinhardtii* exposed to 5×10^{-9} molL^{-1} IHg (MeHg1) and 5×10^{-8} molL^{-1} IHg (MeHg2) (Table S2);

Important features identified by One-way ANOVA and Fisher's post-hoc analysis ($p< 0.05$) in *C. reinhardtii* exposed to 5×10^{-9} molL^{-1} MeHg (MeHg1) and 5×10^{-8} molL^{-1} MeHg (MeHg2) (Table S3); Pathways analysis for IHg exposure (Table S4); Pathways analysis for MeHg exposure (Table S5).

ACKNOWLEDGEMENT

V.I.S. acknowledge the financial support of the Swiss National Science Foundation (Grant IZSEZ0_180186). AK acknowledges the support of U.S. National Science Foundation (Grant NSF 1901515). Any opinions, findings, and conclusions or recommendations expressed in this material are those of the author(s) and do not necessarily reflect the views of the funding agencies.

AUTHORS INFORMATION

Arturo A. Keller ORCID ID 0000-0002-7638-662X

Sanghamitra Majumdar ORCID ID 0000-0002-9525-7620

Vera I. Slaveykova ORCID ID 0000-0002-8361-2509

AUTHOR CONTRIBUTIONS

V.I.S. and A.K. conceived and designed the study. NR performed exposure bioassays and measured Hg in the exposure medium and algae. WwL performed the LC-MS measurements, SM prepared

the samples for metabolomics and overviewed the LC-MS measurements, V.I.S performed analysis and interpretation of metabolomic results, wrote the manuscript, overviewed the overall study. A.K. took part in the data interpretation, manuscript writing, overviewed the overall study. All the authors critically commented and revised the manuscript. All the authors have approved the paper submission.

FUNDING SOURCES

Swiss National Science Foundation (Grant IZSEZ0_180186).

U.S. National Science Foundation (Grant NSF 1901515).

REFERENCES

(1) Sturla, S. J.; Boobis, A. R.; FitzGerald, R. E.; Hoeng, J.; Kavlock, R. J.; Schirmer, K.; Whelan, M.; Wilks, M. F.; Peitsch, M. C., Systems Toxicology: From Basic Research to Risk Assessment. *Chemical Research in Toxicology* **2014,** *27*, (3), 314-329.

(2) Zhang, X.; Xia, P.; Wang, P.; Yang, J.; Baird, D. J., Omics Advances in Ecotoxicology. *Environmental Science & Technology* **2018,** *52*, (7), 3842-3851.

(3) Fiehn, O., Metabolomics – the link between genotypes and phenotypes. *Plant Molecular Biology* **2002,** *48*, (1), 155-171.

(4) Patti, G. J.; Yanes, O.; Siuzdak, G., Metabolomics: the apogee of the omics trilogy. *Nature Reviews Molecular Cell Biology* **2012,** *13*, (4), 263-269.

(5) Johnson, C. H.; Ivanisevic, J.; Siuzdak, G., Metabolomics: beyond biomarkers and towards mechanisms. *Nature Reviews Molecular Cell Biology* **2016,** *17*, (7), 451-459.

(6) Mangal, V.; Nguyen, T. Q.; Fiering, Q.; Gueguen, C., An untargeted metabolomic approach for the putative characterization of metabolites from Scenedesmus obliquus in response to cadmium stress. *Environmental Pollution* **2020,** *266*, 115123.

(7) Samuelsson, L. M.; Larsson, D. G. J., Contributions from metabolomics to fish research. *Molecular BioSystems* **2008,** *4*, (10), 974-979.

(8) Viant, M. R., Recent developments in environmental metabolomics. *Molecular Biosystems* **2008,** *4*, (10), 980-986.

(9) Matich, E. K.; Soria, N. G. C.; Aga, D. S.; Atilla-Gokcumen, G. E., Applications of metabolomics in assessing ecological effects of emerging contaminants and pollutants on plants. *Journal of Hazardous Materials* **2019,** *373*, 527-535.

(10) Majumdar, S.; Keller, A. A., Omics to address the opportunities and challenges of nanotechnology in agriculture. *Critical Reviews in Environmental Science and Technology* **2020**, 1-42.

(11) Gauthier, L.; Tison-Rosebery, J.; Morin, S.; Mazzella, N., Metabolome response to anthropogenic contamination on microalgae: a review. *Metabolomics* **2019,** *16*, (1), 13.

(12) Huang, M.; Keller, A. A.; Wang, X.; Tian, L.; Wu, B.; Ji, R.; Zhao, L., Low Concentrations of Silver Nanoparticles and Silver Ions Perturb the Antioxidant Defense System and Nitrogen Metabolism in N2-Fixing Cyanobacteria. *Environmental Science & Technology* **2020,** *https://doi.org/10.1021/acs.est.0c05300*.

(13) Liu, W.; Majumdar, S.; Li, W.; Keller, A. A.; Slaveykova, V. I., Metabolic perturbations after uptake of silver nanoparticles by freshwater alga Poterioochromonas malhamensis: early detection of stress. *Scientific Reports* **2020,** *10*, 20563.

(14) Driscoll, C. T.; Mason, R. P.; Chan, H. M.; Jacob, D. J.; Pirrone, N., Mercury as a Global Pollutant: Sources, Pathways, and Effects. *Environmental Science & Technology* **2013,** *47*, (10), 4967-4983.

(15) Sakamoto, M.; Murata, K.; Kakita, A.; Sasaki, M., A Review of Mercury Toxicity with Special Reference to Methylmercury. In *Environmental Chemistry and Toxicology of Mercury*, Liu, G.; Cai, Y.; O'Driscoll, N., Eds. 2011; pp 501-516.

(16) Yang, L.; Zhang, Y.; Wang, F.; Luo, Z.; Guo, S.; Strähle, U., Toxicity of mercury: Molecular evidence. *Chemosphere* **2020,** *245*, 125586.

(17) Le Faucheur, S.; Campbell, P. G. C.; Fortin, C.; Slaveykova, V. I., Interactions between mercury and phytoplankton: Speciation, bioavailability, and internal handling. *Environmental Toxicology and Chemistry* **2014,** *33*, (6), 1211-1224.

(18) Dranguet, P.; Flück, R.; Regier, N.; Cosio, C.; Le Faucheur, S.; Slaveykova, V. I., Towards Mechanistic Understanding of Mercury Availability and Toxicity to Aquatic Primary Producers. *CHIMIA International Journal for Chemistry* **2014,** *68*, (11), 799-805.

(19) Cosio, C.; Flück, R.; Regier, N.; Slaveykova, V. I., Effects of macrophytes on the fate of mercury in aquatic systems. *Environmental Toxicology and Chemistry* **2014,** *33*, (6), 1225-1237.

(20) Beauvais-Flück, R.; Slaveykova, V. I.; Cosio, C., Molecular Effects of Inorganic and Methyl Mercury in Aquatic Primary Producers: Comparing Impact to A Macrophyte and A Green Microalga in Controlled Conditions. *Geosciences* **2018,** *8*, 393.

(21) Beauvais-Fluck, R.; Slaveykova, V. I.; Cosio, C., Transcriptomic and physiological responses of the green microalga Chlamydomonas reinhardtii during short-term exposure to subnanomolar methylmercury concentrations. *Environmental Science & Technology* **2016,** *50*, (13), 7126-7134.

(22) Beauvais-Flück, R.; Slaveykova, V. I.; Cosio, C., Cellular toxicity pathways of inorganic and methyl mercury in the green microalga Chlamydomonas reinhardtii. *Scientific Reports* **2017,** *7*, (1), 8034.

(23) Dranguet, P.; Cosio, C.; Le Faucheur, S.; Beauvais-Fluck, R.; Freiburghaus, A.; Worms, I. A. M.; Petit, B.; Civic, N.; Docquier, M.; Slaveykova, V. I., Transcriptomic approach for assessment of the impact on microalga and macrophyte of in-situ exposure in river sites contaminated by chlor-alkali plant effluents. *Water Research* **2017,** *121*, 86-94.

(24) Fernie, A. R.; Stitt, M., On the Discordance of Metabolomics with Proteomics and Transcriptomics: Coping with Increasing Complexity in Logic, Chemistry, and Network Interactions Scientific Correspondence. *Plant Physiology* **2012,** *158*, (3), 1139-1145.

(25) Cajka, T.; Fiehn, O., Toward Merging Untargeted and Targeted Methods in Mass Spectrometry-Based Metabolomics and Lipidomics. *Analytical Chemistry* **2016,** *88*, (1), 524-545.

(26) Harris, E. H., *The Chlamydomonas sourcebook: a comprehensive guide to biology and laboratory use*. Elsevier: 2013.

(27) Puzanskiy, R.; Tarakhovskaya, E.; Shavarda, A.; Shishova, M., Metabolomic and physiological changes of Chlamydomonas reinhardtii (Chlorophyceae, Chlorophyta) during batch culture development. *Journal of Applied Phycology* **2018,** *30*, (2), 803-818.

(28) Davis, M. C.; Fiehn, O.; Durnford, D. G., Metabolic acclimation to excess light intensity in Chlamydomonas reinhardtii. *Plant Cell and Environment* **2013,** *36*, (7), 1391-1405.

(29) Huang, Y.; Li, W.; Minakova, A. S.; Anumol, T.; Keller, A. A., Quantitative analysis of changes in amino acids levels for cucumber (Cucumis sativus) exposed to nano copper. *NanoImpact* **2018,** *12*, 9-17.

(30) Huang, Y.; Adeleye, A. S.; Zhao, L.; Minakova, A. S.; Anumol, T.; Keller, A. A., Antioxidant response of cucumber (Cucumis sativus) exposed to nano copper pesticide: Quantitative determination via LC-MS/MS. *Food Chemistry* **2019,** *270*, 47-52.

(31) Majumdar, S.; Pagano, L.; Wohlschlegel, J. A.; Villani, M.; Zappettini, A.; White, J. C.; Keller, A. A., Proteomic, gene and metabolite characterization reveal the uptake and toxicity mechanisms of cadmium sulfide quantum dots in soybean plants. *Environmental Science-Nano* **2019,** *6*, (10), 3010-3026.

(32) Xia, J.; Wishart, D. S., Web-based inference of biological patterns, functions and pathways from metabolomic data using MetaboAnalyst. *Nature Protocols* **2011,** *6*, 743.

(33) Chong, J.; Wishart, D. S.; Xia, J., Using MetaboAnalyst 4.0 for Comprehensive and Integrative Metabolomics Data Analysis. *Current Protocols in Bioinformatics* **2019,** *68*, (1), e86.

(34) Johnson, W. E.; Li, C.; Rabinovic, A., Adjusting batch effects in microarray expression data using empirical Bayes methods. *Biostatistics* **2006,** *8*, (1), 118-127.

(35) Jung, Y.; Ahn, Y. G.; Kim, H. K.; Moon, B. C.; Lee, A. Y.; Ryu, D. H.; Hwang, G. S., Characterization of dandelion species using 1H NMR- and GC-MS-based metabolite profiling. *Analyst* **2011,** *136*, (20), 4222-4231.

(36) Xia, J.; Wishart, D. S., MSEA: a web-based tool to identify biologically meaningful patterns in quantitative metabolomic data. *Nucleic acids research* **2010,** *38*, (Web Server issue), W71-W77.

(37) Bromke, M. A., Amino Acid Biosynthesis Pathways in Diatoms. *Metabolites* **2013,** *3*, (2), 294-311.

(38) Hildebrandt, Tatjana M.; Nunes Nesi, A.; Araújo, Wagner L.; Braun, H.-P., Amino Acid Catabolism in Plants. *Molecular Plant* **2015,** *8*, (11), 1563-1579.

(39) Vallon, O.; Spalding, M. H., Chapter 4 - Amino Acid Metabolism. In *The Chlamydomonas Sourcebook (Second Edition)*, Harris, E. H.; Stern, D. B.; Witman, G. B., Eds. Academic Press: London, 2009; pp 115-158.

(40) Cosio, C.; Renault, D., Effects of cadmium, inorganic mercury and methyl-mercury on the physiology and metabolomic profiles of shoots of the macrophyte Elodea nuttallii. *Environmental Pollution* **2020,** *257*, 113557.

(41) Less, H.; Galili, G., Principal Transcriptional Programs Regulating Plant Amino Acid Metabolism in Response to Abiotic Stresses. *Plant Physiology* **2008,** *147*, (1), 316-330.

(42) Cullimore, J. V.; Sims, A. P., Glutamine synthetase of Chlamydomonas: its role in the control of nitrate assimilation. *Planta* **1981,** *153*, (1), 18-24.

(43) Matysik, J.; Alia; Bhalu, B.; Mohanty, P., Molecular mechanisms of quenching of reactive oxygen species by proline under stress in plants. *Current Science* **2002,** *82*, (5), 525-532.

(44) Sharma, S. S.; Dietz, K.-J., The significance of amino acids and amino acid-derived molecules in plant responses and adaptation to heavy metal stress. *Journal of Experimental Botany* **2006,** *57*, (4), 711-726.

(45) Taylor, N. L.; Heazlewood, J. L.; Day, D. A.; Millar, A. H., Lipoic acid-dependent oxidative catabolism of alpha-keto acids in mitochondria provides evidence for branched-chain amino acid catabolism in Arabidopsis. *Plant physiology* **2004,** *134*, (2), 838-848.

(46) Johnson, X.; Alric, J., Central Carbon Metabolism and Electron Transport in Chlamydomonas reinhardtii: Metabolic Constraints for Carbon Partitioning between Oil and Starch. *Eukaryotic Cell* **2013,** *12*, (6), 776-793.

(47) Liang, Y.; Kong, F.; Torres-Romero, I.; Burlacot, A.; Cuine, S.; Légeret, B.; Billon, E.; Brotman, Y.; Alseekh, S.; Fernie, A. R.; Beisson, F.; Peltier, G.; Li-Beisson, Y., Branched-Chain

691 Amino Acid Catabolism Impacts Triacylglycerol Homeostasis in Chlamydomonas reinhardtii.
692 *Plant Physiology* **2019,** *179*, (4), 1502-1514.
693 (48) Binder, S.; Knill, T.; Schuster, J., Branched-chain amino acid metabolism in higher plants.
694 *Physiologia Plantarum* **2007,** *129*, (1), 68-78.
695 (49) Antonacci, A.; Lambreva, M. D.; Margonelli, A.; Sobolev, A. P.; Pastorelli, S.; Bertalan,
696 I.; Johanningmeier, U.; Sobolev, V.; Samish, I.; Edelman, M.; Havurinne, V.; Tyystjärvi, E.;
697 Giardi, M. T.; Mattoo, A. K.; Rea, G., Photosystem-II D1 protein mutants of Chlamydomonas
698 reinhardtii in relation to metabolic rewiring and remodelling of H-bond network at QB site.
699 *Scientific Reports* **2018,** *8*, (1), 14745.
700 (50) Lohr, M., Chapter 21 - Carotenoids. In *The Chlamydomonas Sourcebook (Second Edition)*,
701 Harris, E. H.; Stern, D. B.; Witman, G. B., Eds. Academic Press: London, 2009; pp 799-817.
702 (51) Dellero, Y.; Jossier, M.; Schmitz, J.; Maurino, V. G.; Hodges, M., Photorespiratory
703 glycolate–glyoxylate metabolism. *Journal of Experimental Botany* **2016,** *67*, (10), 3041-3052.
704 (52) Timm, S.; Florian, A.; Wittmiß, M.; Jahnke, K.; Hagemann, M.; Fernie, A. R.; Bauwe, H.,
705 Serine acts as a metabolic signal for the transcriptional control of photorespiration-related genes in
706 Arabidopsis. *Plant Physiology* **2013,** *162*, (1), 379-389.
707 (53) Kluender, C.; Sans-Piché, F.; Riedl, J.; Altenburger, R.; Härtig, C.; Laue, G.; Schmitt-
708 Jansen, M., A metabolomics approach to assessing phytotoxic effects on the green alga
709 Scenedesmus vacuolatus. *Metabolomics* **2008,** *5*, (1), 59.
710 (54) Qian, L.; Qi, S.; Cao, F.; Zhang, J.; Zhao, F.; Li, C.; Wang, C., Toxic effects of boscalid on
711 the growth, photosynthesis, antioxidant system and metabolism of Chlorella vulgaris.
712 *Environmental Pollution* **2018,** *242*, 171-181.
713 (55) Booij, P.; Lamoree, M., H. ; Sjollema, S., B.; Voogt, P. d.; Schollee, J., E. ; Vethaak, A. D.;
714 Leonards, P., E. G. , Non-target Metabolomic Profiling of the Marine Microalgae *Dunaliella*

715 *tertiolecta* After Exposure to Diuron using Complementary High- Resolution Analytical
716 Techniques. *Current Metabolomics* **2014,** *2*, (3), 213-222.
717 (56) Matthew, T.; Zhou, W.; Rupprecht, J.; Lim, L.; Thomas-Hall, S. R.; Doebbe, A.; Kruse, O.;
718 Hankamer, B.; Marx, U. C.; Smith, S. M.; Schenk, P. M., The metabolome of Chlamydomonas
719 reinhardtii following induction of anaerobic H2 production by sulfur depletion. *The Journal of*
720 *biological chemistry* **2009,** *284*, (35), 23415-23425.
721 (57) Tietel, Z.; Wikoff, W. R.; Kind, T.; Ma, Y.; Fiehn, O., Hyperosmotic stress in
722 Chlamydomonas induces metabolomic changes in biosynthesis of complex lipids. *European*
723 *Journal of Phycology* **2020,** *55*, (1), 11-29.
724 (58) Zhang, W.; Tan, N. G. J.; Fu, B.; Li, S. F. Y., Metallomics and NMR-based metabolomics
725 of Chlorella sp. reveal the synergistic role of copper and cadmium in multi-metal toxicity and
726 oxidative stress. *Metallomics* **2015,** *7*, (3), 426-438.
727 (59) Zhang, W. L.; Tan, N. G. J.; Li, S. F. Y., NMR-based metabolomics and LC-MS/MS
728 quantification reveal metal-specific tolerance and redox homeostasis in Chlorella vulgaris.
729 *Molecular Biosystems* **2014,** *10*, (1), 149-160.
730 (60) Yong, W.-K.; Sim, K.-S.; Poong, S.-W.; Wei, D.; Phang, S.-M.; Lim, P.-E., Interactive
731 effects of temperature and copper toxicity on photosynthetic efficiency and metabolic plasticity in
732 Scenedesmus quadricauda (Chlorophyceae). *Journal of Applied Phycology* **2018,** *30*, (6), 3029-
733 3041.
734 (61) Gonçalves, S.; Kahlert, M.; Almeida, S. F. P.; Figueira, E., Assessing Cu impacts on
735 freshwater diatoms: biochemical and metabolomic responses of Tabellaria flocculosa (Roth)
736 Kützing. *Science of The Total Environment* **2018,** *625*, 1234-1246.

(62) Bhagavan, N. V.; Ha, C.-E., Chapter 25. Nucleotide Metabolism. In *Essentials of Medical Biochemistry*, Ha, N. V. B. C.-E., Ed. Imprint: Academic Press: 2015; Vol. eBook ISBN: 9780124166974, p 752.

(63) Foyer, C. H.; Noctor, G., Ascorbate and Glutathione: The Heart of the Redox Hub. *Plant Physiology* **2011,** *155*, (1), 2-18.

(64) Grill, E.; Löffler, S.; Winnacker, E.-L.; Zenk, M. H., Phytochelatins, the heavy-metal-binding peptides of plants, are synthesized from glutathione by a specific γ-glutamylcysteine dipeptidyl transpeptidase (phytochelatin synthase). *Proceedings of the National Academy of Sciences* **1989,** *86*, (18), 6838-6842.

(65) Jozefczak, M.; Remans, T.; Vangronsveld, J.; Cuypers, A., Glutathione is a key player in metal-induced oxidative stress defenses. *International Journal of Molecular Sciences* **2012,** *13*, (3), 3145-3175.

(66) Agrawal, S. B.; Agrawal, M.; Lee, E. H.; Kramer, G. F.; Pillai, P., Changes in polyamine and glutathione contents of a green alga, Chlorogonium elongatum (Dang) France exposed to mercury. *Environmental and Experimental Botany* **1992,** *32*, (2), 145-151.

(67) Wu, Y.; Wang, W. X., Intracellular speciation and transformation of inorganic mercury in marine phytoplankton. *Aquatic Toxicology* **2014,** *148*, 122-129.

(68) Gómez-Jacinto, V.; García-Barrera, T.; Gómez-Ariza, J. L.; Garbayo-Nores, I.; Vílchez-Lobato, C., Elucidation of the defence mechanism in microalgae Chlorella sorokiniana under mercury exposure. Identification of Hg–phytochelatins. *Chemico-Biological Interactions* **2015,** *238*, 82-90.

(69) Wu, Y.; Wang, W. X., Thiol compounds induction kinetics in marine phytoplankton during and after mercury exposure. *Journal of Hazardous Materials* **2012,** *217*, 271-278.

(70) Jamers, A.; Blust, R.; De Coen, W.; Griffin, J. L.; Jones, O. A., Copper toxicity in the microalga Chlamydomonas reinhardtii: an integrated approach. *Biometals* **2013,** *18*, 18.

(71) Stoiber, T. L.; Shafer, M. M.; Armstrong, D. E., Differential effects of copper and cadmium exposure on toxicity endpoints and gene expression in Chlamydomonas reinhardtii. *Environmental Toxicology and Chemistry* **2010,** *29*, (1), 191-200.

(72) Jamers, A.; Blust, R.; De Coen, W.; Griffin, J. L.; Jones, O. A. H., An omics based assessment of cadmium toxicity in the green alga Chlamydomonas reinhardtii. *Aquatic Toxicology* **2013,** *126*, 355-364.

(73) Gest, N.; Gautier, H.; Stevens, R., Ascorbate as seen through plant evolution: the rise of a successful molecule? *Journal of Experimental Botany* **2012,** *64*, (1), 33-53.

(74) Smirnoff, N., Ascorbic acid: metabolism and functions of a multi-facetted molecule. *Current Opinion in Plant Biology* **2000,** *3*, (3), 229-235.

(75) Kovacik, J.; Rotkova, G.; Bujdos, M.; Babula, P.; Peterkova, V.; Matus, P., Ascorbic acid protects Coccomyxa subellipsoidea against metal toxicity through modulation of ROS/NO balance and metal uptake. *Journal of Hazardous Materials* **2017,** *339*, 200-207.

(76) Elbaz, A.; Wei, Y. Y.; Meng, Q.; Zheng, Q.; Yang, Z. M., Mercury-induced oxidative stress and impact on antioxidant enzymes in Chlamydomonas reinhardtii. *Ecotoxicology* **2010,** *19*, (7), 1285-1293.

(77) Beauvais-Flück, R.; Slaveykova, V. I.; Cosio, C., Transcriptomic and Physiological Responses of the Green Microalga Chlamydomonas reinhardtii during Short-Term Exposure to Subnanomolar Methylmercury Concentrations. *Environmental Science & Technology* **2016,** *50*, (13), 7126-7134.

(78) Wang, P.; Zhang, B.; Zhang, H.; He, Y. L.; Ong, C. N.; Yang, J., Metabolites change of Scenedesmus obliquus exerted by AgNPs. *Journal of Environmental Sciences* **2019,** *76*, 310-318.

784 (79) Goncalves, S.; Kahlert, M.; Almeida, S. F. P.; Figueira, E., Assessing Cu impacts on
785 freshwater diatoms: biochemical and metabolomic responses of Tabellaria flocculosa (Roth)
786 Kutzing. *Science of the Total Environment* **2018,** *625*, 1234-1246.
787 (80) Weise, S. E.; Weber, A. P. M.; Sharkey, T. D., Maltose is the major form of carbon exported
788 from the chloroplast at night. *Planta* **2004,** *218*, (3), 474-482.
789 (81) Lu, Y.; Sharkey, T. D., The importance of maltose in transitory starch breakdown. *Plant,*
790 *Cell & Environment* **2006,** *29*, (3), 353-366.
791 (82) Hostettler, C.; Kölling, K.; Santelia, D.; Streb, S.; Kötting, O.; Zeeman, S. C., Analysis of
792 starch metabolism in chloroplasts. *Methods Mol Biol* **2011,** *775*, 387-410.
793 (83) Findinier, J.; Tunçay, H.; Schulz-Raffelt, M.; Deschamps, P.; Spriet, C.; Lacroix, J.-M.;
794 Duchêne, T.; Szydlowski, N.; Li-Beisson, Y.; Peltier, G.; D'Hulst, C.; Wattebled, F.; Dauvillée,
795 D., The Chlamydomonas mex1 mutant shows impaired starch mobilization without maltose
796 accumulation. *Journal of Experimental Botany* **2017,** *68*, (18), 5177-5189.
797 (84) Pinto, E.; Sigaud-kutner, T. C. S.; Leitão, M. A. S.; Okamoto, O. K.; Morse, D.; Colepicolo,
798 P., Heavy metal-induced ooxidative stress in algae *Journal of Phycology* **2003,** *39*, (6), 1008-1018.
799 (85) Behzadi Tayemeh, M.; Esmailbeigi, M.; Shirdel, I.; Joo, H. S.; Johari, S. A.; Banan, A.;
800 Nourani, H.; Mashhadi, H.; Jami, M. J.; Tabarrok, M., Perturbation of fatty acid composition,
801 pigments, and growth indices of Chlorella vulgaris in response to silver ions and nanoparticles: A
802 new holistic understanding of hidden ecotoxicological aspect of pollutants. *Chemosphere* **2020,**
803 *238*, 124576.
804 (86) Upchurch, R. G., Fatty acid unsaturation, mobilization, and regulation in the response of
805 plants to stress. *Biotechnology Letters* **2008,** *30*, (6), 967-977.

(87) Filimonova, V.; Gonçalves, F.; Marques, J. C.; De Troch, M.; Gonçalves, A. M. M., Fatty acid profiling as bioindicator of chemical stress in marine organisms: A review. *Ecological Indicators* **2016,** *67*, 657-672.

Supporting information

Metabolomic responses of green alga *Chlamydomonas reinhardtii* exposed to sub-lethal concentrations of inorganic and methylmercury

Vera I. Slaveykova[a,*], Sanghamitra Majumdar[b], Nicole Regier[a], Weiwei Li[b], Arturo A. Keller[b]

[a] University of Geneva, Faculty of Sciences, Earth and Environment Sciences, Department F.-A. Forel for Environmental and Aquatic Sciences, Environmental Biogeochemistry and Ecotoxicology, Uni Carl Vogt, 66 Blvd Carl-Vogt, CH 1211 Geneva, Switzerland

[b] Bren School of Environmental Science & Management, University of California, Santa Barbara, Santa Barbara, California 93106-5131, United States

*corresponding author: vera.slaveykova@unige.ch

LIST OF FIGURES

LIST OF TABLES

Cellular mercury content in alga *C. reinhardtii*

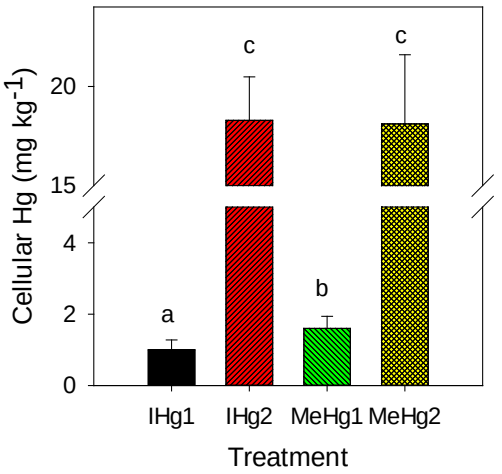

Figure S1. Cellular total mercury accumulated in *C. reinhardtii* exposed to IHg and MeHg for 2h. Different letters show statistical difference between treatments obtained by One way ANOVA followed by Tukey all pairwise comparison test, $p < 0.05$. IHg1: 5×10^{-9} mol L^{-1} IHg, IHg2: 5×10^{-8} mol L^{-1} IHg, MeHg1: 5×10^{-9} mol L^{-1} MeHg, MeHg2: 5×10^{-8} mol L^{-1} MeHg.

Table S1. List of metabolites and the MS parameters for LC-MS targeted metabolomics

Compound	Retention time (min)	Precursor ion (m/z)	Product ions					MLD** µg L^{-1}
			Quant ion (m/z)	Collision energy (V)	Qual ion (m/z)	Collision energy (V)	Fragmentor (V)	
Amino acids								
Alanine	6.61	90.1	44.2	9	45.3	40	40	0.001
Arginine	9.54	175.1	70.1	24	60.1	12	100	0.001
Asparagine	7.31	133.1	87.1	5	74	17	75	0.100
Aspartic acid	8.38	134	88.1	9	74	13	70	0.001
Citrulline	7.89	176.1	159.1	9	70.1	25	80	0.015
Cysteine	5.63	122	59.1	29	76	13	65	0.500
Glutamic acid	7.68	148.1	84.1	17	130	5	75	0.001
Glutamine	7.23	147.1	84.1	17	130.1	9	80	0.050
Glycine	7.00	76	30.3	12	-	-	35	1.500
Histidine	9.06	156.1	110.1	13	83.1	29	90	0.025
Homoserine	6.91	120.1	74.1	9	56.1	21	70	0.015
Isoleucine	3.75	132.1	86.1	9	44.2	25	75	0.001
Leucine	3.38	132.1	86.1	9	30.2	17	75	0.001
Lysine	10.16	147.1	84.1	17	130.1	9	75	0.001
Methionine	4.22	150.1	104	9	56.1	17	75	0.005
Ornithine	10.28	133.1	116	8	70	20	76	0.001
Phenylalanine	2.95	166.1	120.1	13	103	29	80	0.050
Proline	4.96	116.1	70.1	17	43.2	37	75	0.100
Serine	7.26	106.1	88.1	8	42.2	24	67	1.000
Threonine	6.72	120.1	74.1	9	56.1	17	75	0.040
Tryptophan	3.41	205.1	188	8	146	20	80	0.001
Tyrosine	5.01	182.1	136.1	13	91.1	33	85	0.015
Valine	4.95	118.1	72.1	9	55.1	25	70	0.040
Antioxidants								
Glutathione reduced	1.22	308.1	179	12	162	16	91	0.005
2-hydroxycinnamic acid	7.37	163	119.1	12	117.1	28	81	0.001
4-(Trifuoromethyl)cinnamic acid	8.26	215	171.1	12	151.1	20	87	0.000
α-Tocopherol	11.00	431.4	165.1	24	69.1	40	142	0.060
Chlorogenic acid	6.19	353.1	191.1	16	-	-	102	0.001
Curcumin	6.33	367.1	217.1	8	149.1	16	112	0.001
L-Dehydroascorbic acid	8.00	173	158.1	12	-	-	174	0.000
Vanillic acid	6.60	167	152.1	12	108	20	82	50.000
Organic Acids/Phenolics								
Ascorbic acid	2.67	175	114.9	12	-	-	87	0.352
Benzoic acid	5.21	121	77.1	12	-	-	77	0.810
Caffeic acid	4.58	179	135.1	16	-	-	94	0.579
Citric acid	2.17	191	110.8	12	86.9	16	82	3.394

Ferulic acid	5.09	193.1	134.1	16	178.1	12	87	0.340
Fumaric acid	2.67	115	70.9	4	-	-	56	6.793
Gallic acid	2.49	169	125.1	12	79	24	92	1.610
Glutaric acid	2.62	131	86.9	12	112.9	8	71	2.846
Glycolic acid	2.04	75	47	8	72.9	8	46	4.602
Lactic acid	2.23	89.1	43.1	4	-	-	66	6.392
Malic acid	2.07	133	114.9	8	71	16	76	0.516
p-coumaric acid	4.87	163	119.1	16	93.1	36	87	0.342
Pyruvic acid	2.36	87	43.1	4	-	-	66	6.785
Salicyllic acid	5.96	137	93	20	65.1	36	82	0.346
Succinic acid	2.31	117	72.9	12	98.9	8	66	0.382
Amine								
2.4-Diaminoanisole	1.25	139.1	124	16	79	32	71	0.264
2.6-Dimethylaniline	2.18	122.1	105	16	77	32	86	0.459
2-Methyl-5-nitroaniline	2.38	153.1	107	20	89	40	71	1.211
4.4'-Diaminodiphenylmethane	1.27	199.1	106	28	77	40	127	0.145
4.4'-Oxydianiline	1.28	201.1	108	24	80	40	117	1.042
4-Chloroaniline	2.17	128	93	20	75	40	86	1.246
Aniline	1.57	94.1	77	20	51.1	36	40	0.298
Diphenylamine	3.41	170.1	93	28	65.1	36	132	0.527
Ethanolamine	1.23	62.1	44.2	8	45.2	16	66	0.150
m-Phenylenediamine	1.30	109.1	92	16	65	28	76	0.304
o-Anisidine	1.59	124.1	109	16	80	36	61	0.120
o-Toluidine	1.67	108.1	91	20	65	32	91	0.040
Sugar and Sugar Alcohol								
Fructose	1.72	179.1	89	4	-	-	71	2.595
Galactinol	6.17	341.1	179	12	-	-	133	4.360
Glucose/Galactose*	2.19	179.1	89	16	-	-	71	3.072
Lactose	4.57	341.1	161.1	4	-	-	123	22.942
L-fucose	1.35	163.1	89	0	59.1	12	76	3.910
Maltose	4.26	341.1	161.1	4	-	-	123	2.227
Mannose	1.93	179.1	89	16	-	-	71	2.046
Raffinose	6.03	503.2	179	20	221	32	174	1.256
Ribitol/Xylitol*	1.61	151.1	89	8	71.1	16	97	0.646
Ribose	1.18	149	89	4	-	-	76	3.951
Sucrose	3.81	341.1	179	20	-	-	148	1.076
Trehalose	4.79	341.1	179	12	-	-	154	0.647
Xylose/Arabinose*	1.43	149	89	4	-	-	76	3.201
Fatty Acids								
Arachidic acid	7.05	357.3	311.3	4	45.1	32	82	3.351
Heptadecanoic acid	6.14	315.3	269.2	4	45.2	28	76	3.740
Linoleic acid	4.91	325.2	279.1	4	45.1	28	87	2.448
Linolenic acid	4.33	323.2	277.1	4	45.1	40	87	2.663

Myristic acid	4.64	273.2	227.2	4	45.1	8	56	13.633
Palmitic acid	5.70	301.2	255.2	4	45.1	20	36	10.907
Pentadecanoic acid	5.17	287.2	241.2	4	45.1	16	71	12.910
Stearic acid	6.49	329.3	283.2	4	45.1	32	72	7.856
Nucleobase/side/tide								
Adenine	3.08	136.1	119	24	92	32	84	0.872
Adenosine	6.67	268.1	136	20	119	40	84	0.322
AMP	4.84	348.1	136	20	97	32	84	2.900
CMP	2.76	324.1	112	16	95	40	84	0.698
Cytidine	2.90	244.1	112	12	95	40	84	0.643
Cytosine	1.94	112.1	95	20	40.1	20	84	0.656
Guanine	3.34	152.1	135	20	110	24	84	0.326
Guanosine	6.91	284.1	152	12	135	40	84	0.227
Hypoxanthine	5.28	137	110	24	55.1	36	148	0.899
Inosine	6.91	269.1	137	16	110	40	84	0.262
Thymidine	7.28	243.1	127	8	117	8	84	2.504
Thymine	6.71	127.1	110	16	54.1	28	84	1.550
Uracil	3.52	113	70	10	96	20	84	2.792
Uridine	6.33	245.1	113	8	70	40	84	0.578
Xanthine	6.40	153	110	20	55.1	36	84	0.410

*For these 3 pairs of isomers, our LCMS method cannot separate them from each other, thus data shows combined concentration of these isomers.

**MLD: measured limit of detection

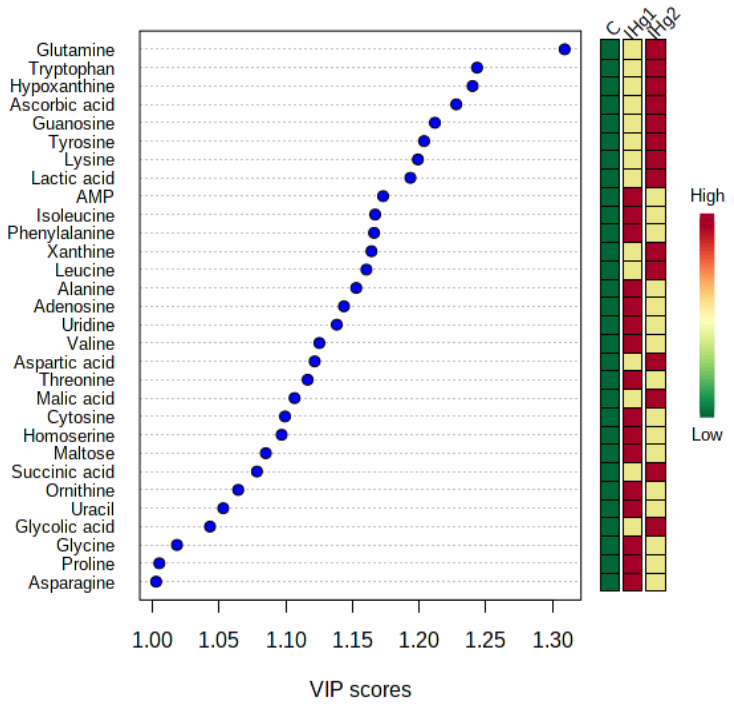

Figure S2. Variable Importance in the Projection (VIP) scores from PLS-DA analysis of discriminating metabolites between unexposed controls and IHg treatments. The colored boxes on the right indicate the relative concentrations of the corresponding metabolite in each group under study. C: untreated control; IHg1: 5×10^{-9} mol L^{-1} IHg; IHg2: 5×10^{-8} mol L^{-1} IHg. Only metabolites with a VIP >1, regarded as significant, are presented.

Table S2. Important features identified by One-way ANOVA and Fisher's post-hoc analysis ($p < 0.05$) in *C. reinhardtii* exposed to 5×10^{-9} mol L^{-1} IHg (IHg1) and 5×10^{-8} mol L^{-1} IHg (IHg2). Data were not normalized or transformed, but autoscaled.

	f.value	p.value	-log10(p)	FDR	Fisher's LSD
Asparagine	154.05	6.9699e-06	5.1568	0.00015433	IHg1 - C; IHg2 - C; IHg1 - IHg2
Valine	133.26	1.0671e-05	4.9718	0.00015433	IHg1 - C; IHg2 – C
AMP	128.56	1.1856e-05	4.926	0.00015433	IHg1 - C; IHg2 – C
Phenylalanine	126.02	1.2572e-05	4.9006	0.00015433	IHg1 - C; IHg2 – C
Lysine	118.29	1.5131e-05	4.8201	0.00015433	IHg1 - C; IHg2 – C
Threonine	105.4	2.1197e-05	4.6737	0.00015547	IHg1 - C; IHg2 – C
Serine	105.16	2.1339e-05	4.6708	0.00015547	IHg1 - C; IHg2 - C; IHg1 - IHg2
Proline	98.476	2.5839e-05	4.5877	0.00016472	IHg1 - C; IHg2 - C; IHg1 - IHg2
Isoleucine	84.573	4.0202e-05	4.3958	0.00022781	IHg1 - C; IHg2 – C
Uridine	79.073	4.8839e-05	4.3112	0.00024908	IHg1 - C; IHg2 – C
Tryptophan	71.065	6.6455e-05	4.1775	0.00027962	IHg1 - C; IHg2 – C
Glycine	70.514	6.7959e-05	4.1678	0.00027962	IHg1 - C; IHg2 – C
Alanine	69.356	7.1276e-05	4.1471	0.00027962	IHg1 - C; IHg2 – C
Hypoxanthine	58.128	0.00011821	3.9274	0.00041862	IHg1 - C; IHg2 – C
Glutamic acid	57.303	0.00012312	3.9097	0.00041862	IHg1 - C; IHg2 - C; IHg1 - IHg2
Adenosine	54.884	0.00013922	3.8563	0.00044376	IHg1 - C; IHg2 – C
Tyrosine	53.268	0.00015156	3.8194	0.00045467	IHg1 - C; IHg2 – C
Leucine	44.199	0.00025678	3.5904	0.00072754	IHg1 - C; IHg2 – C
Xanthine	40.838	0.00032049	3.4942	0.00086025	IHg1 - C; IHg2 – C
Homoserine	39.622	0.0003487	3.4575	0.00088918	IHg1 - C; IHg2 – C
Arginine	36.731	0.00043051	3.366	0.0010455	IHg1 - C; IHg2 - C; IHg1 - IHg2
Glutamine	34.332	0.00051893	3.2849	0.001203	IHg1 - C; IHg2 - C; IHg2 - IHg1
Cytosine	32.907	0.00058322	3.2342	0.0012932	IHg1 - C; IHg2 – C
Histidine	22.958	0.0015436	2.8115	0.0032802	IHg1 - C; IHg2 – C
Uracil	22.586	0.001612	2.7926	0.0032885	IHg1 - C; IHg2 – C
Ascorbic acid	21.89	0.001751	2.7567	0.0034347	IHg1 - C; IHg2 – C
Maltose	20.4	0.0021074	2.6763	0.0039806	IHg1 - C; IHg2 – C
Guanosine	15.884	0.0040095	2.3969	0.0073031	IHg1 - C; IHg2 – C
Aspartic acid	14.169	0.0053351	2.2729	0.0092149	IHg1 - C; IHg2 – C
Ornithine	14.078	0.0054206	2.266	0.0092149	IHg1 - C; IHg2 – C
Palmitic acid	13.54	0.0059675	2.2242	0.0098175	IHg1 - C; IHg2 – C
Citric acid	10.68	0.010546	1.9769	0.016808	IHg1 - C; IHg1 - IHg2
Ethanolamine	10.033	0.012195	1.9138	0.018658	IHg1 - C
Lactic acid	9.9479	0.012438	1.9052	0.018658	IHg1 - C; IHg2 - C
Cytidine	9.0041	0.015609	1.8066	0.02198	IHg1 - C; IHg2 - C
Adenine	8.962	0.015774	1.8021	0.02198	IHg1 - C; IHg2 - C
Citrulline	8.9188	0.015947	1.7973	0.02198	IHg1 - C; IHg2 - C
CMP	8.4613	0.017933	1.7463	0.024016	IHg1 - C; IHg2 - C
Glutathione reduced	8.3707	0.018366	1.736	0.024016	IHg1 - C; IHg2 - C
Stearic acid	6.6995	0.029588	1.5289	0.037725	IHg1 - C; IHg2 - C
Succinic acid	6.3877	0.032635	1.4863	0.040595	IHg1 - C; IHg2 - C
Guanine	6.1396	0.035366	1.4514	0.042944	IHg1 - C; IHg2 - C

Linolenic acid	5.9836	0.03724	1.429	0.044169	IHg1 - C
Linoleic acid	5.891	0.038416	1.4155	0.044527	IHg1 - C
Malic acid	5.4945	0.044051	1.356	0.049925	IHg2 - C

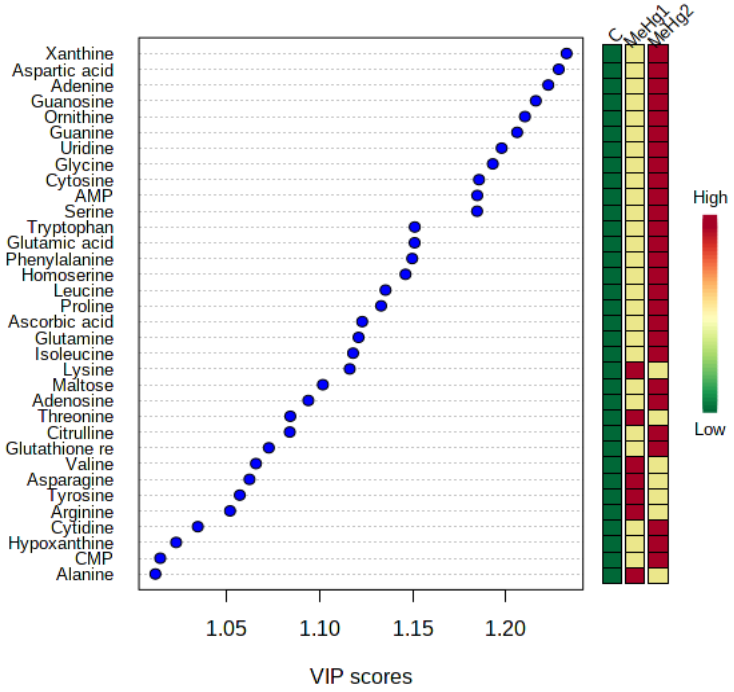

Figure S3. Variable Importance in the Projection (VIP) scores from PLS-DA analysis of discriminating metabolites between unexposed controls and MeHg treatments. The colored boxes on the right indicate the relative concentrations of the corresponding metabolite in each group under study. C: untreated control; MeHg1: 5×10^{-9} mol L^{-1} MeHg; MeHg2: 5×10^{-8} mol L^{-1} MeHg. Only metabolites with a VIP >1, regarded as significant, are shown.

Table S3. Important features identified by One-way ANOVA and Fisher's post-hoc analysis ($p < 0.05$) in *C. reinhardtii* exposed to 5×10^{-9} mol L^{-1} MeHg (MeHg1) and 5×10^{-8} mol L^{-1} MeHg (MeHg2). Data were not normalized or transformed. but autoscaled.

	f.value	p.value	-log10(p)	FDR	Fisher's LSD
Lysine	779.75	5.6298e-08	7.2495	2.8712e-06	MeHg1 - C; MeHg2 - C
Asparagine	165.52	5.642e-06	5.2486	0.00014387	MeHg1 - C; MeHg2 - C
Serine	100.73	2.4193e-05	4.6163	0.00028311	MeHg1 - C; MeHg2 - C
Tyrosine	98.297	2.5976e-05	4.5854	0.00028311	MeHg1 - C; MeHg2 - C
Phenylalanine	94.483	2.9146e-05	4.5354	0.00028311	MeHg1 - C; MeHg2 - C
Homoserine	90.242	3.3307e-05	4.4775	0.00028311	MeHg1 - C; MeHg2 - C
Glycine	75.453	5.5917e-05	4.2525	0.00040739	MeHg1 - C; MeHg2 - C
Cytosine	54.252	0.00014388	3.842	0.00087496	MeHg1 - C; MeHg2 - C
Valine	52.92	0.00015441	3.8113	0.00087496	MeHg1 - C; MeHg2 - C
Isoleucine	50.004	0.00018132	3.7416	0.00092474	MeHg1 - C; MeHg2 - C
Proline	45.043	0.00024349	3.6135	0.0010113	MeHg1 - C; MeHg2 - C
Threonine	44.43	0.00025305	3.5968	0.0010113	MeHg1 - C; MeHg2 - C
Glutamic acid	43.462	0.0002692	3.5699	0.0010113	MeHg1 - C; MeHg2 - C
Tryptophan	42.988	0.0002776	3.5566	0.0010113	MeHg1 - C; MeHg2 - C
AMP	41.416	0.00030814	3.5112	0.0010477	MeHg1 - C; MeHg2 - C
Guanosine	36.937	0.00042387	3.3728	0.0012982	MeHg1 - C; MeHg2 - C
Uridine	36.662	0.00043274	3.3638	0.0012982	MeHg1 - C; MeHg2 - C
Leucine	33.65	0.00054846	3.2609	0.001554	MeHg1 - C; MeHg2 - C
Xanthine	32.308	0.00061339	3.2123	0.0016465	MeHg1 - C; MeHg2 - C; MeHg2 - MeHg1
Guanine	29.66	0.00077499	3.1107	0.0019762	MeHg1 - C; MeHg2 - C
Alanine	27.971	0.00090886	3.0415	0.002127	MeHg1 - C; MeHg2 - C
Arginine	27.247	0.00097568	3.0107	0.002127	MeHg1 - C; MeHg2 - C
Ascorbic acid	26.991	0.0010009	2.9996	0.002127	MeHg1 - C; MeHg2 - C
Adenine	26.991	0.0010009	2.9996	0.002127	MeHg1 - C; MeHg2 - C; MeHg2 - MeHg1
Ornithine	25.838	0.0011258	2.9485	0.0022966	MeHg2 - C; MeHg2 - MeHg1
Aspartic acid	22.512	0.001626	2.7889	0.0031894	MeHg1 - C; MeHg2 - C; MeHg2 - MeHg1
Glutathione reduced	16.119	0.0038634	2.413	0.0072975	MeHg1 - C; MeHg2 - C
Adenosine	14.147	0.0053552	2.2712	0.009754	MeHg1 - C; MeHg2 - C
Maltose	12.734	0.0069318	2.1592	0.012085	MeHg1 - C; MeHg2 - C
Uracil	12.602	0.0071089	2.1482	0.012085	MeHg1 - C; MeHg2 - C
Histidine	11.914	0.0081398	2.0894	0.013391	MeHg1 - C; MeHg2 - C
Succinic acid	11.636	0.0086115	2.0649	0.013725	MeHg1 - C; MeHg2 - C
Glycolic acid	9.749	0.01303	1.8851	0.020137	MeHg1 - C; MeHg2 - C
Palmitic acid	9.3923	0.014187	1.8481	0.021281	MeHg1 - C; MeHg2 - C
Glutamine	8.5937	0.017326	1.7613	0.025246	MeHg1 - C; MeHg2 - C
Citrulline	8.0991	0.019747	1.7045	0.027975	MeHg1 - C; MeHg2 - C
Hypoxanthine	7.7384	0.021805	1.6615	0.030055	MeHg1 - C; MeHg2 - C

Table S4. Pathways analysis for IHg exposure. Total is the total number of compounds in the pathway; Hits is the actually matched number from the user uploaded data; Raw p is the original p value calculated from the enrichment analysis; Holm p is the p value adjusted by Holm-Bonferroni method; FDR p is the p value adjusted using False Discovery Rate; Impact is the pathway impact value calculated from pathway topology analysis.

	Total	Expected	Hits	Raw p	-log(p)	Holm adjust	FDR	Impact
Aminoacyl-tRNA biosynthesis	48	1.9301	18	6.4993e-15	32.667	5.4594e-13	5.4594e-13	0.16667
Arginine biosynthesis	17	0.68357	6	2.6942e-05	10.522	0.0022362	0.0011316	0.37499
Glycine, serine and threonine metabolism	28	1.1259	6	0.00058557	7.4429	0.048016	0.016396	0.46291
Alanine, aspartate and glutamate metabolism	20	0.8042	5	0.00083194	7.0918	0.067387	0.017471	0.77586
Purine metabolism	65	2.6136	8	0.0032625	5.7252	0.261	0.054811	0.13707
Glyoxylate and dicarboxylate metabolism	31	1.2465	5	0.0065315	5.0311	0.51599	0.087081	0.30286
Lysine biosynthesis	11	0.44231	3	0.0080095	4.8271	0.62474	0.087081	0
Valine, leucine and isoleucine biosynthesis	21	0.84441	4	0.0082934	4.7923	0.63859	0.087081	0
Glutathione metabolism	27	1.0857	4	0.02037	3.8937	1	0.19012	0.46987
Arginine and proline metabolism	31	1.2465	4	0.032469	3.4275	1	0.27274	0.34805
Phenylalanine, tyrosine and tryptophan biosynthesis	22	0.88462	3	0.054844	2.9033	1	0.41881	0.02182
Pyrimidine metabolism	38	1.528	4	0.062065	2.7796	1	0.43446	0.18404
Nitrogen metabolism	11	0.44231	2	0.069067	2.6727	1	0.44628	0
Sulfur metabolism	14	0.56294	2	0.10592	2.245	1	0.62572	0.03548
Linoleic acid metabolism	3	0.12063	1	0.11594	2.1547	1	0.62572	1
Cyanoamino acid metabolism	15	0.60315	2	0.11919	2.1271	1	0.62572	0
Tropane. piperidine and pyridine alkaloid biosynthesis	4	0.16084	1	0.15158	1.8866	1	0.70738	0
Betalain biosynthesis	4	0.16084	1	0.15158	1.8866	1	0.70738	0
Valine, leucine and isoleucine degradation	37	1.4878	3	0.18305	1.698	1	0.72705	0
Isoquinoline alkaloid biosynthesis	5	0.20105	1	0.18582	1.683	1	0.72705	0.58333
beta-Alanine metabolism	20	0.8042	2	0.19042	1.6585	1	0.72705	0
Citrate cycle (TCA cycle)	20	0.8042	2	0.19042	1.6585	1	0.72705	0.12311
Carbon fixation in photosynthetic organisms	21	0.84441	2	0.20534	1.5831	1	0.74992	0
Pantothenate and CoA biosynthesis	22	0.88462	2	0.22039	1.5124	1	0.77135	0
Cysteine and methionine metabolism	43	1.729	3	0.24727	1.3973	1	0.8086	0
Phenylalanine metabolism	7	0.28147	1	0.25028	1.3852	1	0.8086	0.375
Monobactam biosynthesis	8	0.32168	1	0.28061	1.2708	1	0.87302	0
Butanoate metabolism	10	0.4021	1	0.33772	1.0855	1	1	0
Nicotinate and nicotinamide metabolism	12	0.48252	1	0.39038	0.94063	1	1	0
Selenocompound metabolism	16	0.64336	1	0.48371	0.72627	1	1	0
alpha-Linolenic acid metabolism	16	0.64336	1	0.48371	0.72627	1	1	0.13043

Ascorbate and aldarate metabolism	17	0.68357	1	0.50476	0.68367	1	1	0
Sphingolipid metabolism	18	0.72378	1	0.52498	0.6444	1	1	0
Histidine metabolism	18	0.72378	1	0.52498	0.6444	1	1	0.09651
Tyrosine metabolism	18	0.72378	1	0.52498	0.6444	1	1	0.37255
Fatty acid elongation	21	0.84441	1	0.5809	0.54318	1	1	0
Pyruvate metabolism	21	0.84441	1	0.5809	0.54318	1	1	0
Propanoate metabolism	21	0.84441	1	0.5809	0.54318	1	1	0
Starch and sucrose metabolism	21	0.84441	1	0.5809	0.54318	1	1	0.1025
Thiamine metabolism	22	0.88462	1	0.59806	0.51406	1	1	0
Fatty acid biosynthesis	52	2.0909	2	0.63026	0.46162	1	1	0
Tryptophan metabolism	28	1.1259	1	0.68752	0.37467	1	1	0.1875
Fatty acid degradation	36	1.4476	1	0.7771	0.25219	1	1	0
Glycerophospholipid metabolism	36	1.4476	1	0.7771	0.25219	1	1	0.01173
Porphyrin and chlorophyll metabolism	54	2.1713	1	0.89672	0.10901	1	1	0

Table S5. Pathways analysis for MeHg exposure. Total is the total number of compounds in the pathway; Hits is the actually matched number from the user uploaded data; Raw p is the original p value calculated from the enrichment analysis; Holm p is the p value adjusted by Holm-Bonferroni method; FDR p is the p value adjusted using False Discovery Rate; the Impact is the pathway impact value calculated from pathway topology analysis.

	Total	Expected	Hits	Raw p	-log(p)	Holm adjust	FDR	Impact
Aminoacyl-tRNA biosynthesis	48	1.6364	18	1.7253e-16	36.296	1.4493e-14	1.4493e-14	0.16667
Arginine biosynthesis	17	0.57955	6	9.9598e-06	11.517	0.00082666	0.00041831	0.37499
Glycine, serine and threonine metabolism	28	0.95455	6	0.00022965	8.379	0.018831	0.0064302	0.46291
Alanine. aspartate and glutamate metabolism	20	0.68182	5	0.00037796	7.8807	0.030614	0.0079371	0.77586
Purine metabolism	65	2.2159	8	0.0010598	6.8496	0.084787	0.017805	0.13707
Valine, leucine and isoleucine biosynthesis	21	0.71591	4	0.0045492	5.3928	0.35939	0.060069	0
Lysine biosynthesis	11	0.375	3	0.0050058	5.2972	0.39045	0.060069	0
Glutathione metabolism	27	0.92045	4	0.011504	4.465	0.88584	0.1208	0.46987
Glyoxylate and dicarboxylate metabolism	31	1.0568	4	0.018693	3.9796	1	0.15702	0.27619
Arginine and proline metabolism	31	1.0568	4	0.018693	3.9796	1	0.15702	0.34805
Phenylalanine. tyrosine and tryptophan biosynthesis	22	0.75	3	0.036026	3.3235	1	0.25855	0.02182
Pyrimidine metabolism	38	1.2955	4	0.036935	3.2986	1	0.25855	0.18404
Nitrogen metabolism	11	0.375	2	0.051302	2.97	1	0.33149	0
Sulfur metabolism	14	0.47727	2	0.079615	2.5306	1	0.47769	0.03548
Cyanoamino acid metabolism	15	0.51136	2	0.089932	2.4087	1	0.50362	0
Valine, leucine and isoleucine degradation	37	1.2614	3	0.12824	2.0539	1	0.60531	0
Tropane. piperidine and pyridine alkaloid biosynthesis	4	0.13636	1	0.12971	2.0425	1	0.60531	0
Betalain biosynthesis	4	0.13636	1	0.12971	2.0425	1	0.60531	0
beta-Alanine metabolism	20	0.68182	2	0.14645	1.9211	1	0.63793	0
Carbon fixation in photosynthetic organisms	21	0.71591	2	0.15851	1.842	1	0.63793	0
Isoquinoline alkaloid biosynthesis	5	0.17045	1	0.15948	1.8358	1	0.63793	0.58333
Pantothenate and CoA biosynthesis	22	0.75	2	0.17076	1.7675	1	0.64831	0
Cysteine and methionine metabolism	43	1.4659	3	0.17751	1.7287	1	0.64831	0
Phenylalanine metabolism	7	0.23864	1	0.21608	1.5321	1	0.75628	0.375
Monobactam biosynthesis	8	0.27273	1	0.24297	1.4148	1	0.81638	0
Butanoate metabolism	10	0.34091	1	0.29408	1.2239	1	0.9501	0
Nicotinate and nicotinamide metabolism	12	0.40909	1	0.34182	1.0735	1	1	0
Selenocompound metabolism	16	0.54545	1	0.42805	0.84851	1	1	0
Ascorbate and aldarate metabolism	17	0.57955	1	0.44783	0.80335	1	1	0
Sphingolipid metabolism	18	0.61364	1	0.46693	0.76157	1	1	0
Histidine metabolism	18	0.61364	1	0.46693	0.76157	1	1	0.09651
Tyrosine metabolism	18	0.61364	1	0.46693	0.76157	1	1	0.37255

Citrate cycle (TCA cycle)	20	0.68182	1	0.50324	0.68669	1	1	0.03273
Fatty acid elongation	21	0.71591	1	0.52047	0.65302	1	1	0
Propanoate metabolism	21	0.71591	1	0.52047	0.65302	1	1	0
Starch and sucrose metabolism	21	0.71591	1	0.52047	0.65302	1	1	0.1025
Thiamine metabolism	22	0.75	1	0.53713	0.62152	1	1	0
Tryptophan metabolism	28	0.95455	1	0.62583	0.46867	1	1	0.1875
Fatty acid degradation	36	1.2273	1	0.71876	0.33023	1	1	0
Fatty acid biosynthesis	52	1.7727	1	0.84211	0.17185	1	1	0
Porphyrin and chlorophyll metabolism	54	1.8409	1	0.85319	0.15877	1	1	0

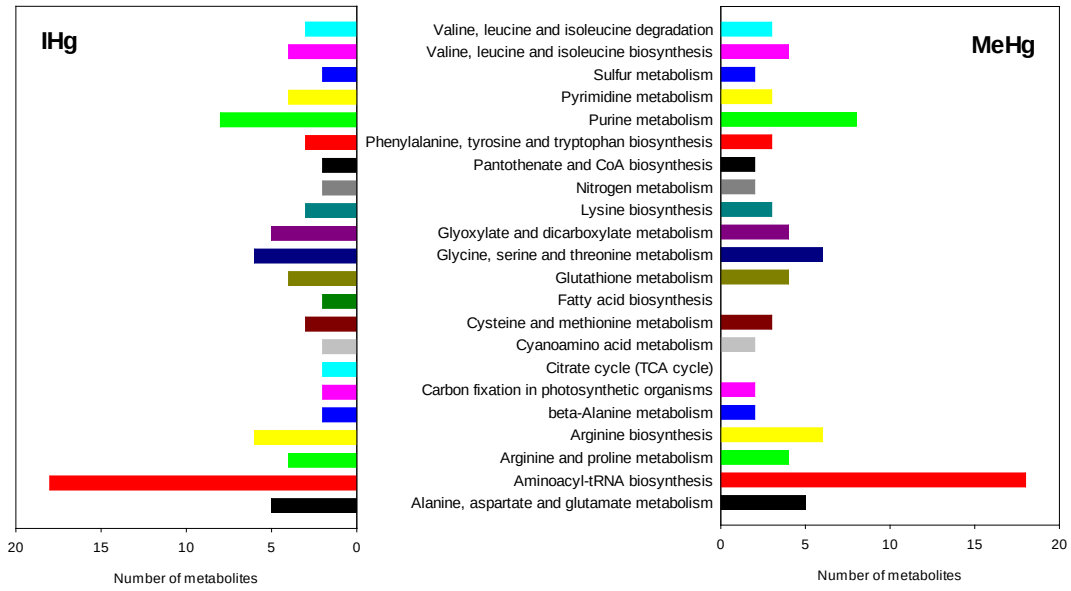

Figure S4. Metabolic pathways from KEGG with at least 2 significantly altered metabolites by IHg or MeHg exposure.

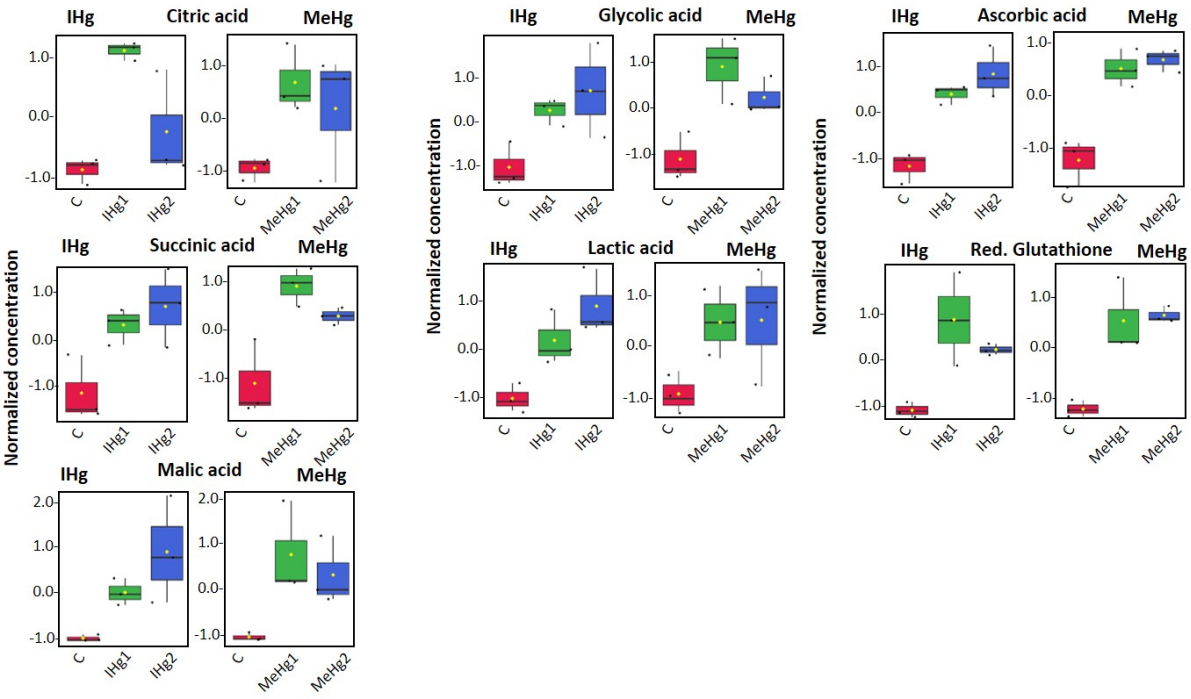

Figure S5. Box plots of relative abundance of metabolites involved in carboxylic acid metabolism and antioxidants. *C. reinhardtii* was treated for 2h with 5×10^{-9} mol L^{-1} IHg (IHg1), 5×10^{-8}M mol L^{-1} IHg (IHg2), 5×10^{-9} mol L^{-1} MeHg (MeHg1), 5×10^{-8} mol L^{-1} MeHg (MeHg2); unexposed control (C).

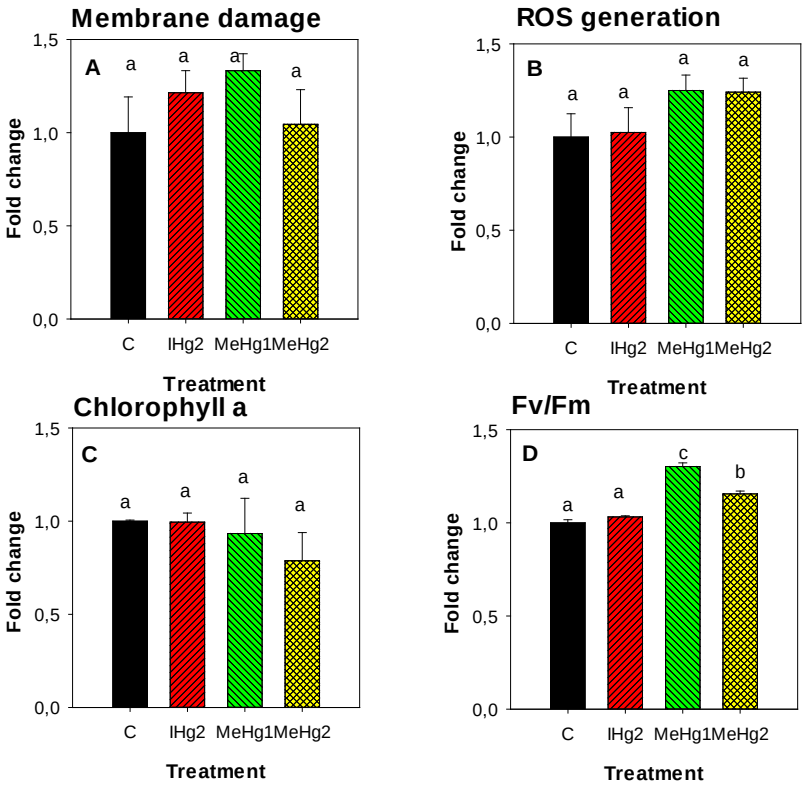

Figure S6. Effect of IHg and MeHg exposure on physiology of *C. reinhardtii*. (a) membrane damage, assessed by propidium iodine stain and FCM; (B): Reactive oxygen species (ROS) generation determined by CellROX®Green stain and flow cytometry; (C) chlorophyll a; (D) Maximum quantum yield of photosystem II (Fv/Fm). Fold change is calculated as a ratio of the respective effects observed in Hg - treated cells and untreated control. Different numbers show statistical difference between treatments obtained by One-way ANOVA followed by Tukey all pairwise comparison test ($p < 0.05$). C: unexposed control, IHg2: 7×10^{-8} mol L^{-1} IHg; MeHg1: 7×10^{-9} mol L^{-1} MeHg; MeHg2: 7×10^{-8} mol L^{-1} MeHg. The figure is prepared based on the data published in Ref. [1].

Two-hour exposure of *C. reinhardtii* to 7×10^{-9} mol L^{-1} MeHg and 7×10^{-8} mol L^{-1} IHg or MHg resulted in no significant changes in the percentage of the cell with the enhanced ROS and damaged membrane, suggesting that the antioxidant system of the algal cells is able to cope with the mercury compounds induced stress. Chlorophyll a content was not altered by the exposure to IHg or MeHg, however the photosynthesis efficiency was significantly increased for 7×10^{-9} mol L^{-1} MeHg and 7×10^{-8} mol L^{-1} MeHg exposure concentrations with respect to the control.

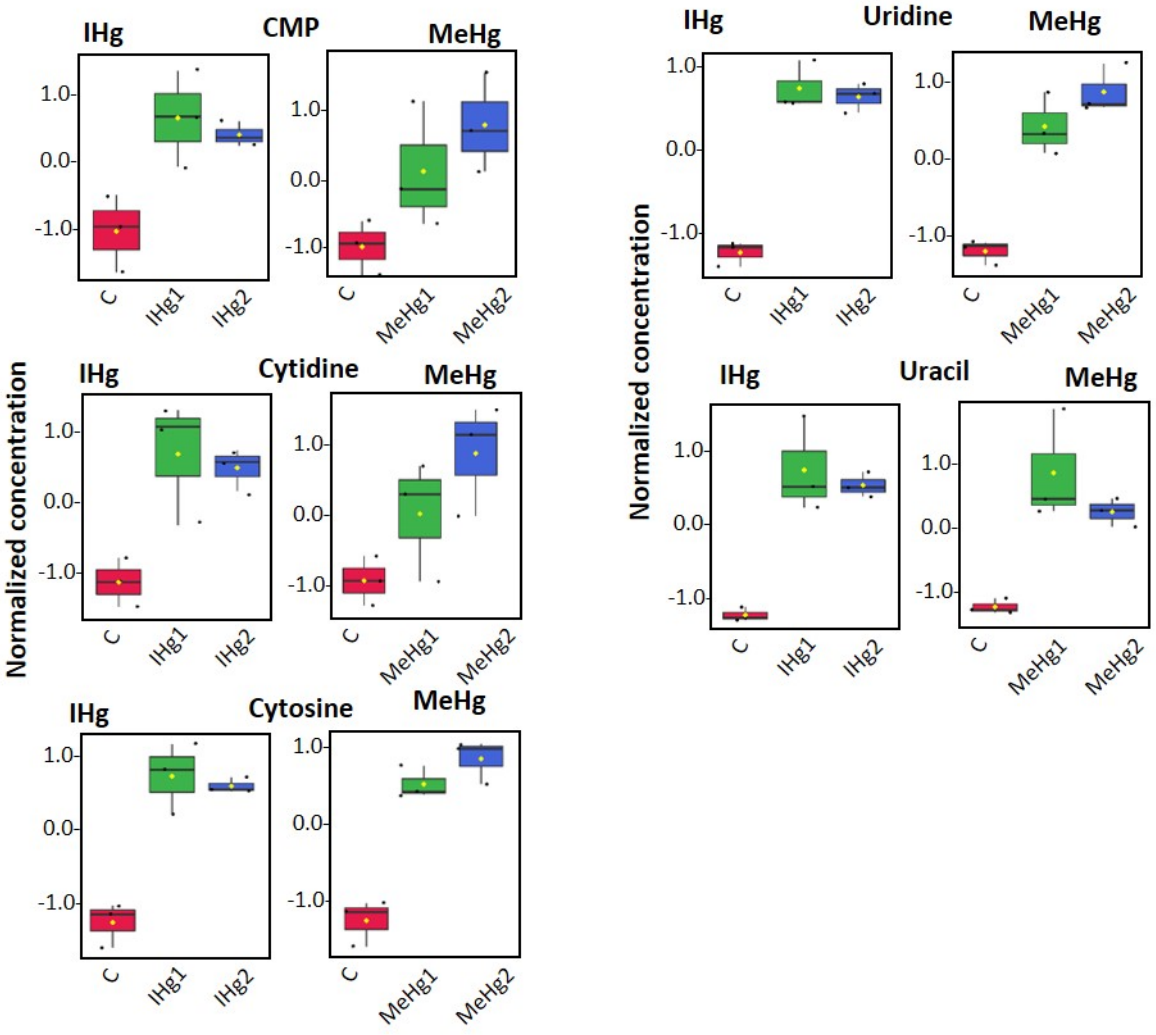

Figure S7. Box plots of relative abundance of nucleobase/tides/sides of pyrimidine metabolism. *C. reinhardtii* was treated for 2h with 5×10^{-9} mol L^{-1} IHg (IHg1), 5×10^{-8}M mol L^{-1} IHg (IHg2), 5×10^{-9} mol L^{-1} MeHg (MeHg1), 5×10^{-8} mol L^{-1} MeHg (MeHg2); unexposed control (C).

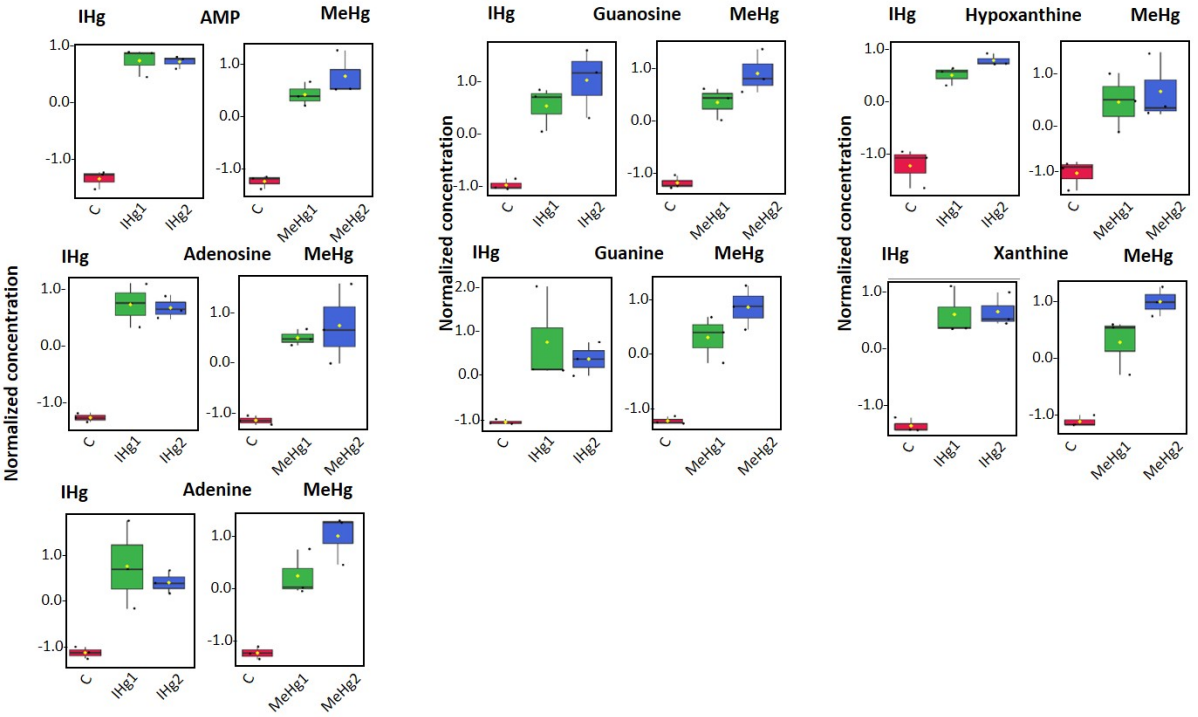

Figure S8. Box plots of relative abundance of nucleobase/tides/sides of purine metabolism. *C. reinhardtii* was treated for 2h with 5×10^{-9} mol L^{-1} IHg (IHg1), 5×10^{-8} mol L^{-1} IHg (IHg2), 5×10^{-9} mol L^{-1} MeHg (MeHg1), 5×10^{-8} mol L^{-1} MeHg (MeHg2); unexposed control (C).

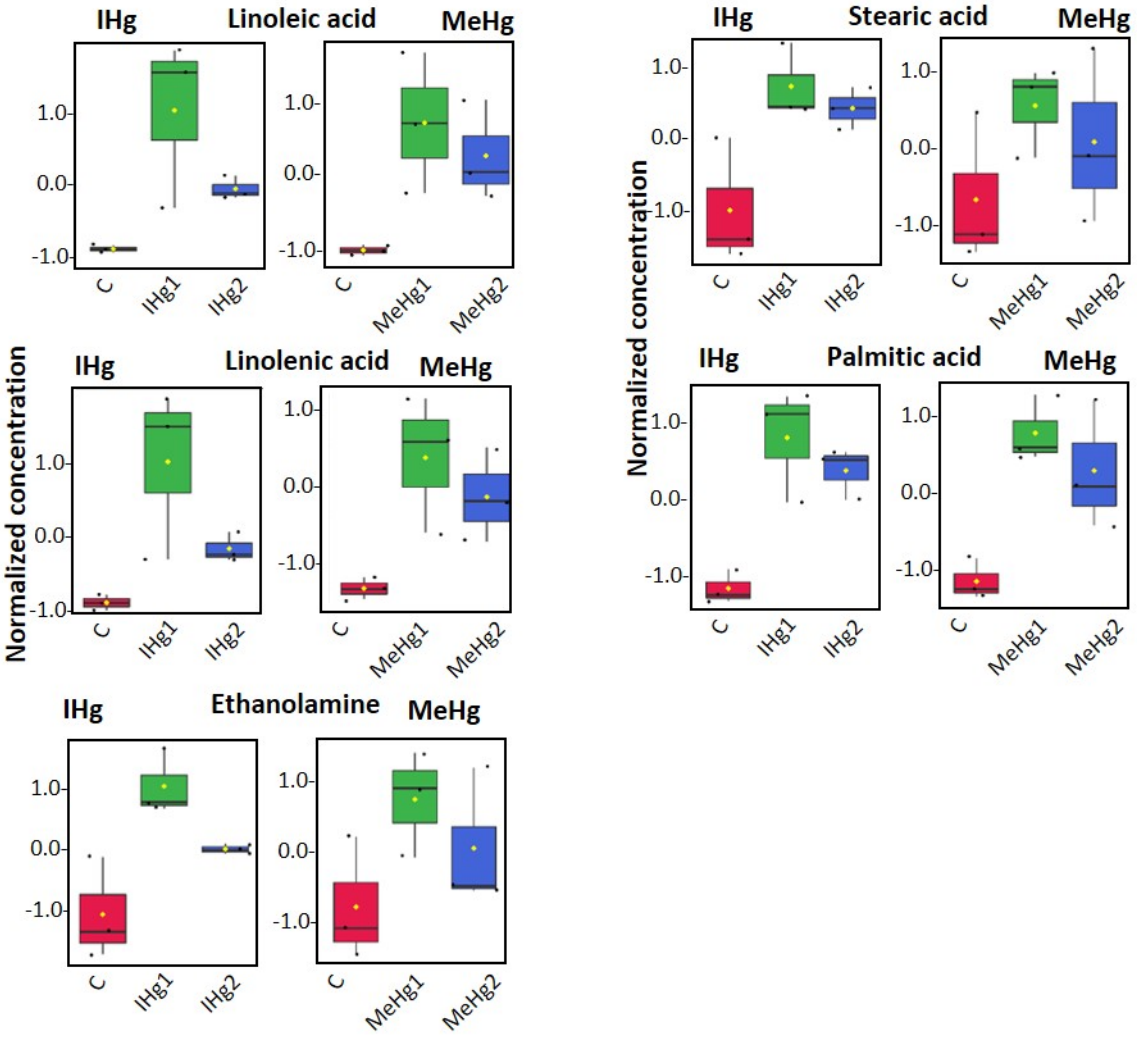

Figure S9. Box plots of relative abundance of metabolites involved in fatty acids metabolism and ethanolamine. *C. reinhardtii* was treated for 2h with 5×10^{-9} mol L^{-1} IHg (IHg1), 5×10^{-8} mol L^{-1} IHg (IHg2), 5×10^{-9} mol L^{-1} MeHg (MeHg1), 5×10^{-8} mol L^{-1} MeHg (MeHg2); unexposed control (C). The changes in the abundance of ethanolamine, linoleic acid, linolenic acid and stearic acid in MeHg exposure were not significantly different from the unexposed control ($p > 0.05$).

(1) Beauvais-Flück, R.; Slaveykova, V. I.; Cosio, C., Cellular toxicity pathways of inorganic and methyl mercury in the green microalga Chlamydomonas reinhardtii. *Scientific Reports* **2017,** *7*, (1), 8034.